2006-08-31

Detection of Proteins by Two-Photon Excitation of Native Fluorescence

Li Li
Brigham Young University - Provo

DETECTION OF PROTEINS BY TWO-PHOTON EXCITATION OF NATIVE FLUORESCENCE

by

Li Li

A thesis submitted to the faculty of

Brigham Young University

In partial fulfillment of the requirements for the degree of

Master of Science

Department of Chemistry and Biochemistry

Brigham Young University

December 2006

BRIGHAM YOUNG UNIVERSITY

GRADUATE COMMITTEE APPROVAL

of a thesis submitted by

Li Li

This thesis has been read by each member of the following graduate committee and by majority vote has been found to be satisfactory.

_____	_____
Date	Paul B. Farnsworth, Chair
_____	_____
Date	Milton L. Lee
_____	_____
Date	Adam T. Woolley
_____	_____
Date	Steven W. Graves

BRIGHAM YOUNG UNIVERSITY

As chair of the candidate's graduate committee, I have read the thesis of Li Li in its final form and have found that (1) its format, citations, and bibliographical style are consistent and acceptable and fulfill university and department style requirements; (2) its illustrative materials including figures, tables, and charts are in place; and (3) the final manuscript is satisfactory to the graduate committee and is ready for submission to the university library.

_____ _____

Date

Paul B. Farnsworth
Chair, Graduate Committee

Accepted for the Department

_____

David V. Dearden
Graduate Coordinator

Accepted for the College

_____

Thomas W. Sederberg
Associate Dean, College of Physical and Mathematical Sciences

ABSTRACT

DETECTION OF PROTEINS BY TWO-PHOTON EXCITATION OF NATIVE FLUORESCENCE

Li Li

Department of Chemistry and Biochemistry

Master of Science

Proteins are of primary importance to the structure and function of all living cells. Study of proteins relies on the ability to separate a complex mixture so that individual proteins can be more easily processed by other techniques. Since protein samples often exist at low concentration in a small volume, the trend in chemical analysis is toward micro total analysis systems (μTAS) or lab-on-a-chip devices. Among μTAS separation methods, the relatively new electric field gradient focusing (EFGF) technique has shown potential. It focuses and separates analytes based on their electrophoretic migration in an opposing hydrodynamic flow. The detection principles that are compatible with μTAS separation may not always scale down. This thesis represents the development of laser-induced two-photon fluorescence detection on a microchip separation device.

This detection is based on excitation of native fluorescence of aromatic amino acids by simultaneous absorption of two photons. First, a compact two-photon prototype

detector was investigated. Its sensitivity was improved after discovery of the source of the background and subsequent reduction of background levels. Simple CE separation on a square capillary was coupled to this detector to demonstrate its ability for micro-scale detection. However, this detector did not provide a way to view the location illuminated by a laser and was difficult to use for on-microchip detection. A two-photon microscope was constructed on the frame of a commercial Olympus microscope to solve this problem. The eyepiece of this microscope enabled viewing of the detection volume, and the removal of a glass compensator from the trinocular head allowed for UV detection. This detection system was carefully aligned and optimized before coupling to microchip CE. Two microchip substrates including poly (methyl methacrylate) (PMMA) and glass, and two chip layouts were explored for their compatibilities with the microscope detector. It was found that the PMMA chip with conventional chip layout was not suitable for two-photon detection; therefore, a novel chip layout on PMMA was designed. Through testing the new design, it was concluded that precise focusing of the laser was essential to successful detection on microchips. Although the precise focusing of the laser inside microchip channels was not achieved completely in the limited research period, it is believed that this new design should be an appropriate solution to coupling PMMA chips with the two-photon microscope. Finally, glass chips were employed to successfully demonstrate the detection of amino acids.

ACKNOWLEDGMENTS

I would first like to express my sincere gratitude to the Department of Chemistry and Biochemistry at Brigham Young University (BYU). The department has provided me the opportunity to study at BYU as a Master's student and supported me with tuition and teaching assistantships. I also appreciate the financial assistance from the National Institutes of Health.

I gratefully appreciate the mentorship of my academic advisor, Dr. Farnsworth, during my graduate studies. Thanks to Dr. Lee, Dr. Woolley, and Dr. Graves for serving on my committee. I appreciate their valuable assistance, especially, on capillary electrophoresis and separation. I am also indebted to my colleagues, Dr. Jeff Macedone and Uchenna Paul.

Finally, I express my deepest appreciation to my parents in China and my husband, Bo Zhang. Their love was a great support for me to complete my Master's degree.

TABLE OF CONTENTS

Page

LIST OF FIGURES

Page

Chapter 1

Detection Methods for Microfabricated Devices

1.1 Introduction

"Micro-total analysis systems" (μ-TAS) have been extensively used for chemical analysis since the first introduction of the concept in 1989.[1] In general, μ-TAS refers to chip-based analytical microdevices that employ short and narrow micromachined channels for separations, such as chromatography, electrophoresis, electro-chromatography, and separations in immunochemical assays. Not only separations, but other analytical procedures, such as sample pretreatment and detection, can potentially be included on a small microchip. Capillary electrophoresis (CE) performed in capillary channels of glass-made chips was one of the earliest examples of μ-TAS.[2] The authors reported separation of fluorescently labeled amino acids with up to 75,000 theoretical plates in about 15 seconds, and separation with 600 plates was completed within 4 seconds. Since the first paper demonstrating the promising analytical potential for miniaturized devices, numerous descriptions of separations in microfabricated channels have been published.[3-5]

Among these separations, equilibrium gradient techniques have attracted interest more recently. The most appeal of these techniques arise from their ability to analyze biological samples where the analytes are in a wide range of concentration. As one of the equilibrium gradient techniques, electric field gradient focusing (EFGF) has been under

development.[6] In this technique, charged analytes are focused at the point in the separation channel where their electrophoretic velocities are equal to the opposing hydrodynamic flow. Two recent papers have described the application of EFGF on microchips. Kelly *et al*[7] carried out protein focusing in a μEFGF device and concluded that this device offered 3-fold better resolution compared than capillary-based systems. Liu *et al*[8] reported a novel fabrication method for μEFGF devices and achieved protein separation and selective elution of specific proteins.

However, a reduction in size of the microchips in which separations are performed results in increased demands on detection systems. For example, the sample volume in conventional microchips is in the pL range and the optical path length is as short as a few micrometers. Thus, highly sensitive methods are needed to detect very low concentrations of samples. Absorbance detectors are the most commonly used detectors, since most molecules absorb UV light at 195-210 nm.[9] However, the pathlength dependency of absorbance gives low sensitivities for small sized microchip channels, and access to UV wavelengths may become problematic due to absorbance by microchip materials. Electrochemical detection has attracted great interest in recent years because the detectors can be microfabricated on the chip, creating an overall system that is compact and compatible with the concept of μ-TAS.[10-11] In general, in this method, the chemical signal is directly converted into the electronic domain through simple electrodes and then detected.

Laser-induced fluorescence (LIF) has been the most widely used detection

method for microchip separations because of its high sensitivity for small volume detection and its suitability for biomolecules. One of the first demonstrations of single-molecule detection in a capillary using LIF was reported by Peck *et al.* in 1989.[12] They used a 514.5 nm argon-ion laser to excite the fluorescence of B-phycoerythrin (PE) in a 8-μm-diameter capillary and achieved single-molecule detection The application of single-molecule detection in a microchip was first reported in 1997 by Effenhauser.[13] The authors combined chip-based microfluidic devices made of poly (dimethylsiloxane) (PDMS) with a LIF detector, which enabled them to perform electrophoresis experiments on the level of single DNA molecules with >50% detection efficiency. In the work by Effenhauser and many other groups, fluorescence detection was based on an argon-ion laser with an emission line at 488 nm. Excitation at 488 nm requires biomolecules, such as amino acids, peptides and proteins, to be labeled with fluorescent tags. Although, from the standpoint of detection, labeling results in high sensitivity, the complicated chemistry and time-consuming procedures associated with analyte derivatization may lead to some adverse effects.

Alternatively, native fluorescence has been used increasingly as the detection method for biomolecules. In particular, proteins containing tryptophan, tyrosine, and phenylalanine fluoresce when they are excited in the range of 250 nm to 300 nm. Swaile and Sepaniak were the first to demonstrate native fluorescence with on-column detection using UV excitation (frequency-doubled Ar-ion laser, 257 nm).[14] Using the same laser wavelength, Nie *et al*. achieved detection limits in the range of $(3 - 15) \times 10^{-20}$ mol for

native fluorescence detection of polycyclic aromatic hydrocarbons in CE.[15] On the other hand, Lee and Yeung showed that the detection limits of native, tryptophan-, or tyrosine-containing proteins can be < 10^{-9} M by using a 275 nm Argon-ion laser.[16] Following this work, they then demonstrated the first use of native fluorescence to detect catecholamines in CE by using a 284 nm frequency-doubled Kr ion laser and reported a subnanomolar detection limit of 7×10^{-10} M. [17]

Most previous studies on native fluorescence detection are based on single-photon excitation (SPE). However, SPE still has several shortcomings. First, conventional SPE requires special UV optics. Second, in SPE, the emission wavelength is close to the laser excitation wavelength on the longer wavelength side. Thus, Raman scattering, the most significant background in fluorescence, often overlaps with fluorescence signals, and other background from scattering off flow cell walls may become dominant.

These problems can be overcome by the introduction of two-photon excitation (TPE), in which a molecule can absorb two long-wavelength photons to reach the first singlet excited state as in SPE. TPE was first predicted by Mayer in 1931 in her doctoral dissertation.[18] However, it was not observed until lasers were invented around 1960. This is because the molecules must absorb two photons nearly simultaneously, normally within 10^{-15}-10^{-16} s.[19] This condition can only be achieved by laser sources that have high local intensities. Kaiser and Garrett first generated blue TPE light by illuminating CaF_2:Eu^{2+} crystals with a ruby optical laser in 1961.[20] Later, Singh and Bradley detected three-photon absorption in single crystals of naphthalene excited by a ruby laser and

estimated the absorption cross section of naphthalene crystals.[21] Subsequently, multiphoton excitation and fluorescence has been used in molecular spectroscopy to study various materials, especially in the area of biology.

One of the earliest biological applications of TPE was done by Jiang *et al.*[22] in 1984. They recorded the fluorescence spectra of albumin, apohemoglobin, hemoglobin and tryptophan after TPE at 532 nm using a Nd:YAG laser. They also showed that the origin of the fluorescence emission of these proteins in TPE arose from tryptophan residues. However, TPE was not widely used until the early 1990s, which may be partly due to the inherently low signals associated with the process. Several papers have discussed the improved detection limits in two-photon spectroscopy. The success of these approaches relies on the ability to separate the linear and nonlinear components of fluorescence. Fisher and Lytle[23] demonstrated that spatial filtering of two-photon excited fluorescence in combination with second harmonic detection improved detection limits significantly. A detection limit of 7.55 nM was obtained for the laser dye coumarin-480 (S/N=3) with an 82 MHz train of 1-ps pulses having an average power of 650 mW. At the same time, the Roeraade group[24] in Sweden reported the use of a frequency-doubled blue laser to detect naphthalene-2,3-dicarboxaldehyde (NDA) in CE and obtained a detection limit of 0.9 amol. Rehms and Callis[25] studied the TPE spectra of the three aromatic amino acids and pointed out that TPE spectra of phenylalanine and tyrosine were quite different from their SPE spectra and both were blue-shifted relative to SPE. Tryptophan was the strongest of the three and its TPE spectrum was similar in shape and relative magnitude

to SPE. The biological application of TPE boomed after the invention of two-photon laser scanning microscopy (TPLSM) by Denk, Strickler, and Webb in 1990.[26,27] Since then, TPLSM is widely used for the study of three-dimensional (3D) and dynamic properties of biological systems.

In this thesis, microchip CE has been extensively used as a microfluidic test platform for TPE fluorescence testing in preparation for eventual application to EFGF. The microchip had a simple cross-column configuration, which was the first chip design and has been widely used since its introduction. It consisted of a straight separation channel intersected by a second channel for sample injection. This configuration was best for high-speed electrophoretic separations without considering separation efficiency.[28]

This thesis describes progress in development of two-photon LIF detection for microfluidic separations. Chapter 2 describes efforts in improving the sensitivity of a prototype TPE fluorescence detector. Capillary electrophoresis separation of amino acids was performed using a square capillary to provide evidence for feasibility of microchannel detection. Chapter 3 describes a two-photon microscope setup and characterization. The microscope provides a precise way to detect inside the microfluidic channel. In chapter 4, the application of the two-photon microscope is demonstrated by detecting amino acids in a microchip separation device. Chapter 5 summarizes conclusions resulting from this thesis work and provides recommendations for further work.

1.2 References

1. Manz, A.; Becker, H. (Eds) *Microsystem Technology in Chemistry and Life Science*, Springer Verlag, Berlin **1998**
2. Harrison, D.J.; Fluri, K.; Seiler, K.; Fan, Z.; Effenhauser, C.S.; Manz, A. *Science*, **1993**, *261*, 895-897
3. Hutt, L.D.; Glavin, D.P.; Bada, J.L.; Mathies, R.A. *Anal. Chem.* **1999**, *71*, 4000-4006
4. Jacobson, S.D.; Culbertson, C.T.; Daler, J.E.; Ramsey, J.M. *Anal. Chem*. **1998**, *70*, 3476-3480
5. Wallenborg, S.R.; Bailey, C.G. *Anal. Chem*. **2000**, *72*, 1872-1878
6. Humble, P.; Kelly, R.; Woolley, A.; Tolley, H.; Lee, M. *J. Chromatogr.* **2003**, *76*, 5641-5648
7. Kelly, R.; Li, Y.; Woolley, A. *Anal. Chem.* **2006**, *78*, 2565-2570
8. Liu, J.; Sun, X.; Farnsworth, P.; Lee, M. *Anal. Chem.* **2006**, *78*, 4654-4662
9. Swinney, K.; Bornhop, D.J. *Electrophoresis* **2000**, *21*, 1239-1250
10. Fanguy, J.; Henry, C. *Electrophoresis* **2002**, *23*, 767-773
11. Galloway, M.; Stryjewski, W.; Henry, A.; Ford, S.; Llopic, S.; McCarley, R.; Soper, S. *Anal. Chem*. **2003**, *74*, 2407-2415
12. Peck, K.; Stryer, L.; Glazer, A.; Mathies, R. *Proc. Natl. Acad. Sci. USA* **1989**, *86*, 4087-4091
13. Effenhauser, C.S.; Bruin, G.J.M.; Paulus, A.; Ehrat, M. *Anal. Chem*. **1997**, *69*, 3451-3457

14. Swaile, D.F.; Sepaniak, M.J. *J. Liq. Chromatogr.* **1991**, *14*, 869-889

15. Nie, S.; Dadoo, R.; Zare, R.N. *Anal. Chem*. **1993**, *65*, 3571-3575

16. Lee, T.T.; Yeung, E.S. *J. Chromatogr*. **1992**, *595*, 319-325

17. Chang, H.; Yeung, E.S. *Anal. Chem*. **1995**, *67*, 1079-1083

18. Goppert-Mayer, M. *Ann. Phys.* **1931**, *9*

19. Lakowicz, J.R. Principles of Fluorescence Spectroscopy, 2nd ed.; Kluwer Academic: New York, **1999**; pp 57-59

20. Kaiser, W.; Garrett, C.G.B. *Phys. Rev. Tech.* **1961**, *7*, 229-231

21. Singh, S.; Bradley, L.T. *Phys. Rev. Tech.* **1964**, *12*, 612-614

22. Jiang, S; Lian, S.; Ruan, K; Hui, L.; Liu, S.; Zhang, Z.; Li, Q. *Chem. Phys. Let*. **1984**, *104*, 109-111

23. Fisher, W.G.; Lytle, F.E. *Anal. Chem*. **1993**, *65*, 631-635

24. Jansson, M.; Roeraade J. *Anal. Chem*. **1993**, *65*, 2766-2769

25. Rehms, A.A.; Callis, P.R. *Chem. Phys. Lett*. **1993**, *208*, 276-282

26. Xu, C.; Zipfel, W.; Shear, J.B.; Williams, R.M.; Webb, W.W. *Proc. Natl. Acad. Sci. USA* **1996**, *93*, 10763-10768

27. Denk, W.; Strickler, J.H.; Webb, W.W. *Science* **1990**, *248*, 73

28. Bruin, G.J.M. *Electrophoresis* **2000**, *21*, 3931-3951

Chapter 2

Improvement and Characterization of a Prototype Two-photon Detector

2.1 Introduction

The detection of proteins is of great interest since proteins are of fundamental importance to human health.[1-3] There has been a remarkable growth in the use of fluorescence spectroscopy, and it has become an essential research tool to study proteins.[4] As mentioned in Chapter 1 of this thesis, TPE has appeared as an alternative detection method which overcomes the problems created by single-photon excitation (SPE), such as the need of deep UV lasers and UV transparent materials, and the overlap of Raman scattering. TPE of native fluorescence also overcomes difficulties in labeling the analytes, which usually complicates sample preparation and detection.[5-7]

Because TPE requires photon flux densities on the order of 10^{31} photons/cm^2·s,[8] powerful sources, usually lasers, are used to excite the two-photon fluorescence. Okerberg and Shear[9] used a femtosecond (fs) mode-locked titanium: sapphire (Ti:S) oscillator pumped by a solid-state frequency doubled neodymium:vanadate ($Nd:YVO_4$) laser to detect the intrinsic fluorescence of aromatic amino acids and achieved detection limits at the amol level. Lippitz *et al.*[10] observed single protein molecules by exciting their intrinsic tryptophan emission after TPE. The laser they used was an argon-ion/titanium-sapphire pumped frequency doubled 180 fs laser. Femtosecond lasers are

useful tools for obtaining low detection limits for proteins. However, such lasers are large and expensive, and usually cost over $100,000, characteristics that limit their use in routine methods for protein detection in most analytical labs.

In this thesis, a compact and inexpensive two-photon detector for proteins based on a microchip laser is described, whose longest dimension is less than 6 inches and costs only about $6,000. The size and cost of this laser satisfy the requirements for detectors for μ-TAS. Characterization of such a detector was done by measuring the detection limits of three aromatic amino acids and a protein in both static and pumped flow systems. Capillary electrophoresis (CE) was also performed to separate a sample mixture.

2.2 Prototype TPE Detector

The prototype TPE detector was built by a previous graduate student, Uchenna P. Paul, in our lab. The detailed setup process and optics considerations can be found in Uchenna P. Paul's thesis.[11] Here, I just give a brief description of the detector optics. The detector consists of the following main components: a microchip laser, a beam expander, a dichroic mirror, a microscope objective, a tube lens, a photodiode, and a photomultiplier tube (PMT). Figure 2-1 shows the schematic setup of the detector and Figure 2-2 is a photograph of the detector.

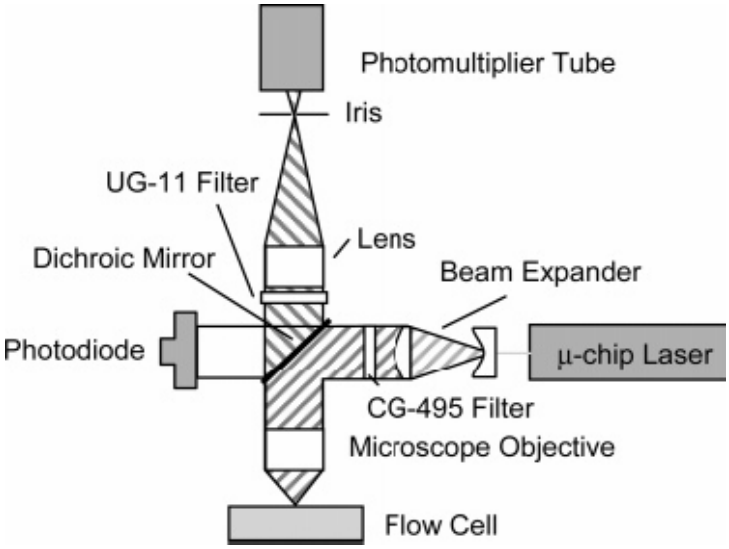

Figure 2-1. Schematic setup of the two-photon prototype detector (from Ref. 12). The 532 nm laser beam is expanded 20 times by a beam expander after emission from a diode pumped laser, transmitted by a CG-495 filter, reflected by a dichroic mirror positioned at 45^{o} with respect to the source radiation, and focused into a flow cell by a microscope objective. The fluorescence emission is collected by the same objective, transmitted through the dichroic mirror, a UG-11 filter, a tube lens, and focused on a PMT through an aperture. A small amount of laser beam passing through the dichroic mirror and hitting on the photodiode acts as a trigger for fluorescence signal detection.

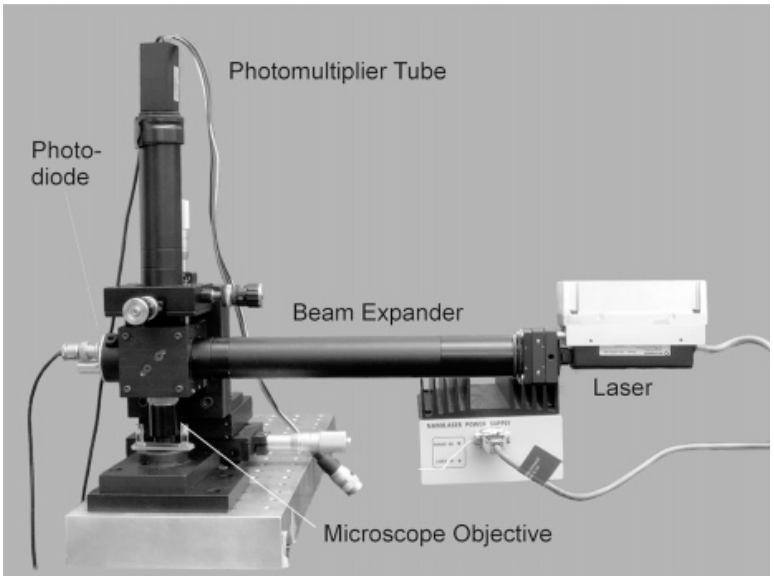

Figure 2-2. Photograph of the two-photon prototype detector (from Ref. 12).

The key component of the detector was a diode-pumped solid state nanolaser (JDS Uniphase, San Jose, CA). The average power of the laser was 29.3 mW. The pulses generated by the laser had the width of 0.5 ns and repetition rate of 6.56 kHz. If one assumed a rectangular pulse shape, these parameters corresponded to a peak power of 8.9 kW. The arrangement of the optics was called epi-geometry, which meant that excitation and emission were transferred by the same objective. Compared to the conventional 90^{o}-geometry, epi-geometry offered some practical advantages.[13] First, the experimental alignment was much easier due to fewer optics. Second, considering that the application of our detector was toward microchips, which usually had a small working area, having fewer optical components made arranging the optics much simpler.

The laser beam was expanded 20 times by a beam expander. The beam expander consisted of a planoconvex and a planoconcave lens, both being anti-reflection coated at 532 nm. The calculated magnification of the beam expander was 20. For a 0.2 mm initial laser beam diameter, the expanded beam had a diameter of 4 mm. The dichroic mirror played an important role in epi-geometry fluorescence detection. In our case, the dichroic mirror reflected >99.5% of the excitation laser beam at 532 nm and transmitted >85% of the fluorescence emission in the range of 280-400 nm. The microscope objective (LMU-20X-UVB, OFR, Caldwell, NJ) used in this detector had a design wavelength range of 193 nm to 450 nm and anti-reflection coating from 240 nm to 360 nm. These wavelengths were well matched for fluorescence emission, but a poor match for the 532 nm laser. According to Uchenna Paul's work, 50% reflection losses for the laser were

estimated due to 12 optical surfaces of the objective. The laser radiation was outside the achromatic range of the objective and, thus, the fluorescence was not directly coming from the focal point of the laser excitation.[12]

The UG-11 filter, located between the dichroic mirror and tube lens, had two transmission windows. One transmitted from 250 to 400 nm, another from 650 to 800 nm. The fluorescence emission passed through the filter and the scattered laser beam at 532 nm was absorbed. It should be pointed out that the UG-11 filter had a small transmission window in the infrared, which required that the PMT should not respond to the infrared light. The fluorescence-focusing lens (also called "tube lens") was an air-spaced achromatic doublet with focal length of 100 mm. The focused light was passed through a 1-mm iris and detected with a compact photomultiplier tube (Model H6780-03, Hamamatsu, Bridgewater, NJ). A small amount of the laser beam passing through the dichroic mirror and hitting the photodiode (DET 210, Thorlabs, Newton, NJ) acted as a trigger for data acquisition and signal processing electronics because the laser was free running. The signal collected by the PMT was first amplified by an amplifier (Model 310, Sonoma Instruments, Santa Rosa, CA), which was connected through a coaxial delay line to either a gated photon counter (SR400, Stanford Research, Sunnyvale, CA) or a gated integrator (SR250, Stanford Research). Gated detection was important in the two-photon detection system because it effectively rejected the dark current from the PMT. For example, with the gate width set to 34 ns, the measurement duty cycle was 2.2×10^{-4} for the 6.56 kHz laser, and dark current was reduced to negligible levels. The gate delay was

set to match the rising edge of the gate with the rising edge of the laser pulse.[12]

2.2.1 Background Discovery

The CG-495 filter was not added to the detector until coworkers and I found that there was a background component in this system that was within the bandpass of the UG-11 filter and could be detected by the PMT. Because Uchenna Paul's work had determined that the background was not due to the auto-fluorescence of the UG-11 filter, we suspected it was caused by the laser itself. Therefore, the following experiment was performed and the source of the background was discovered.

Figure 2-3 shows the schematic experimental setup for the purpose of discovering the source of the background from the laser. The expanded laser beam was introduced through the entrance slit of a monochromator and hit on the monochromator grating. The light was dispersed by the grating and passed through the same UG-11 filter that was used in the two-photon detector. The filter was placed outside the exit slit of the monochromator and the transmitted light was detected by an H6780-03 PMT. The monochromator was then set to scan from 350 to 360 nm. The scanning result (Figure 2-4) showed a narrow peak centered at 355 nm, which confirmed our suspicion that the third harmonic from the YAG laser generated in the doubling optics was the source of the background. A W2-CG-GG-495-1.00-2.5-532-0 long pass filter purchased from CVI Laser was placed just after the beam expander to prevent the 355 nm radiation from

reaching the sample. This filter absorbed light shorter than 495 nm and was anti-reflection coated at 532 nm.

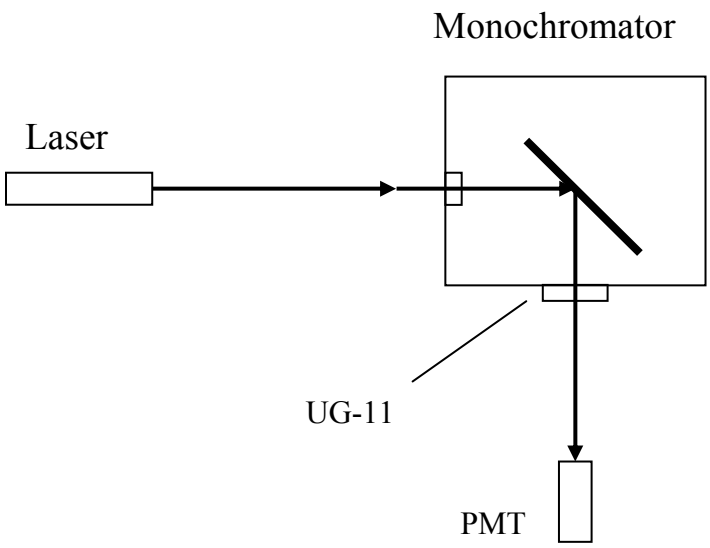

Figure 2-3. Schematic setup of the experiment designed for determination of source of laser background

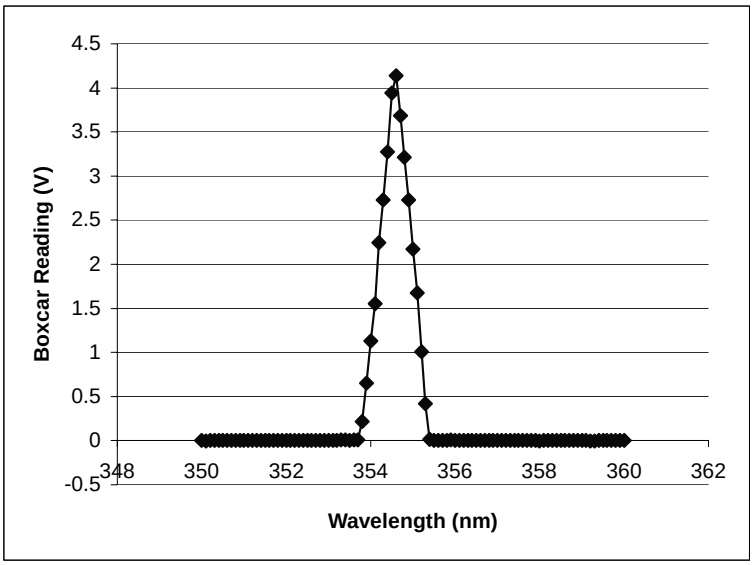

Figure 2-4. Spectrum from 350 nm to 360 nm resulting from the background experiment diagrammed in Figure 2-3.

2.2.2 Detection Limits Determination of Aromatic Amino Acids (Static & Pumped Flow Systems)

After the removal of the third harmonic from the laser, the detector was characterized by determining the detection limits for three aromatic amino acids, tryptophan, tyrosine, and phenylalanine, and a protein, bovine serum albumin (BSA), a 69 kDa protein containing 3 tryptophans, 21 tyrosines, and 30 phenylalanines.[14]

First, samples were studied under static flow conditions in a 1.0-mm quartz flow cell (NSG Precision Cells, Farmingdale, NY). Stock solutions of 1×10^{-2} M of DL-tryptophan (Matheson, Coleman & Bell, Norwood, Ohio), 1×10^{-3} M of tyrosine (ICN Biomedicals, Irvine, CA), 1×10^{-2} M of phenylalanine (Aldrich, Milwaukee, WI), and 1×10^{-4} M of BSA were prepared in 10 mM pH 7.0 phosphate buffer. The buffer was prepared from $NaH_2PO_4\cdot H_2O$ (CCI, Columbus, OH) and $Na_2HPO_4\cdot 12H_2O$ (Baker, Phillipsburg, NJ) dissolved in 18 MΩ water from a Milli-Q water system (Millipore, Billerica, MA). For each of the four analytes, a series of five or six dilutions of the stock solution was prepared to make the calibration curves. Figures 2-5 to 2-8 show the calibration curves for tryptophan, tyrosine, phenylalanine, and BSA, respectively. Each concentration point in the calibration curves represents an average of 20 data points taken with one-second integration using a photon counter. For the blank (phosphate buffer), 200 data points were taken to determine the average and the standard deviation of the background. The detection limits, calculated from the slopes of the calibration curves and

three times the standard deviation of the blank, were 1.0 μM, 8.2 μM, 87 μM, and 0.24 μM, respectively.

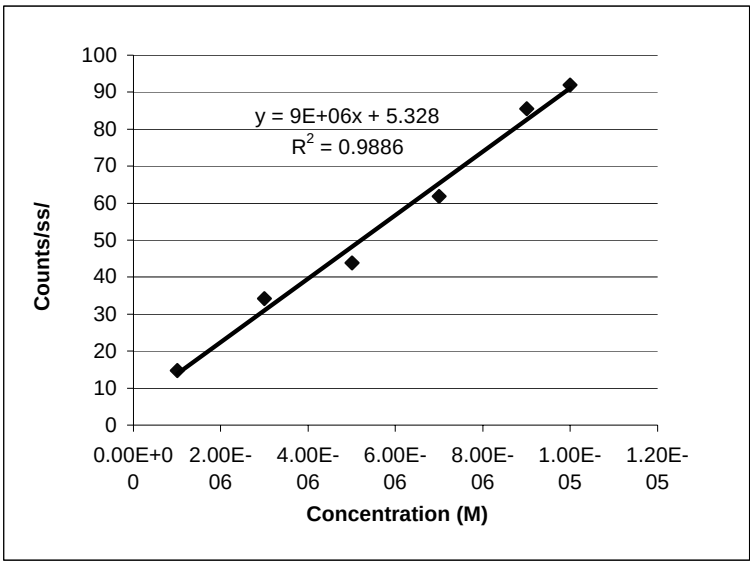

Figure 2-5. Calibration curve for tryptophan. A detection limit of 1.0 μM was calculated at three times the standard deviation of the blank.

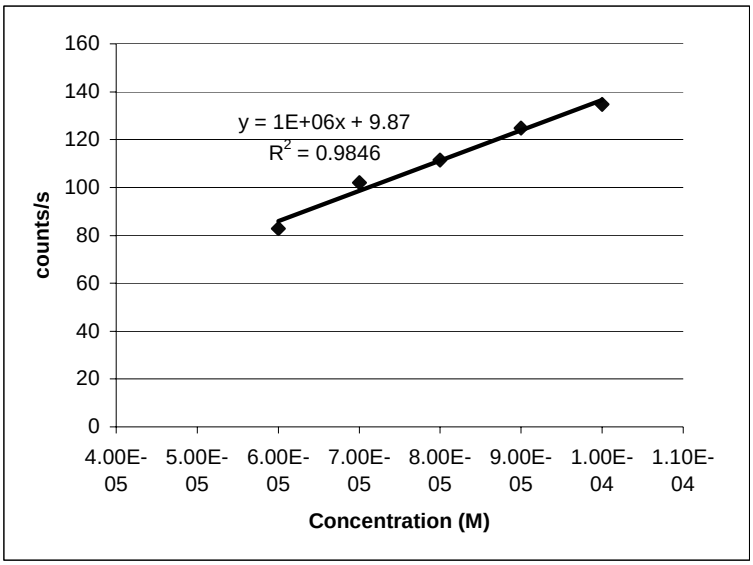

Figure 2-6. Calibration curve for tyrosine. A detection limit of 8.2 μM was calculated at three times the standard deviation of the blank.

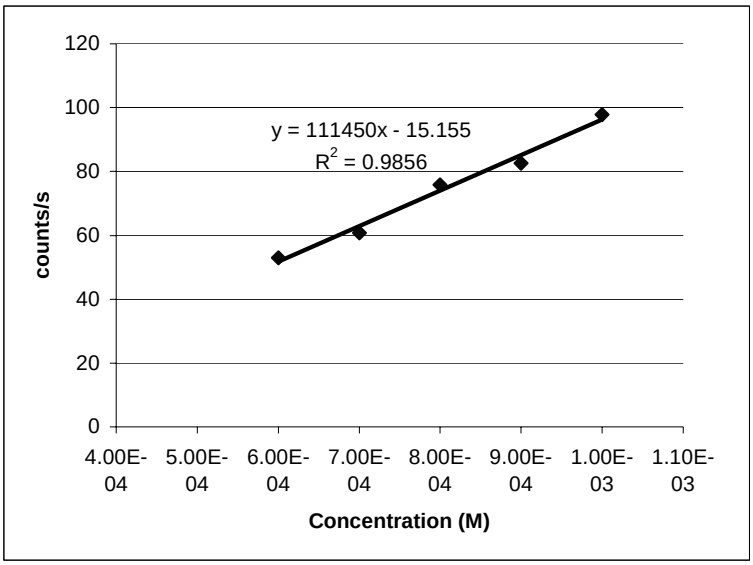

Figure 2-7. Calibration curve for phenylalanine. A detection limit of 87 μM was calculated at three times the standard deviation of the blank.

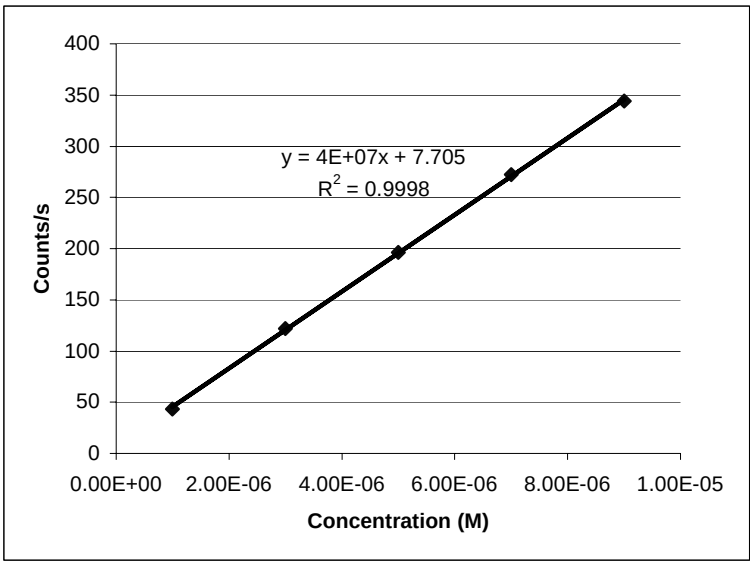

Figure 2-8. Calibration curve for BSA. A detection limit of 0.24 μM was calculated at three times the standard deviation of the blank.

Next, samples were pumped through the flow cell by a syringe pump set at a rate of 2.0 mL/min, which was the optimized rate to give maximized signals. The detection limits obtained in this way were 0.47 μM for tryptophan, 2.0 μM for tyrosine, 62 μM for phenylalanine, and 0.13 μM for BSA. Figures 2-9 to 2-12 show the calibration curves for these experiments.

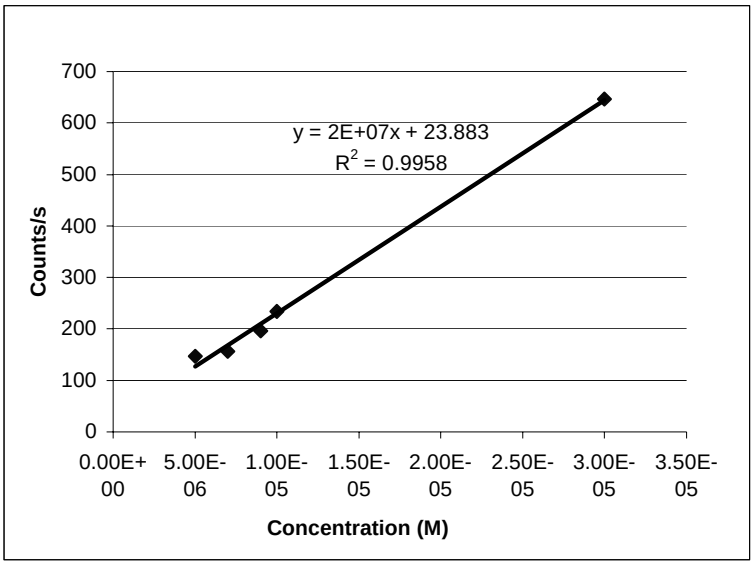

Figure 2-9. Calibration curve for tryptophan under pumped flow conditions. A detection limit of 0.47 μM was calculated at three times the standard deviation of the blank.

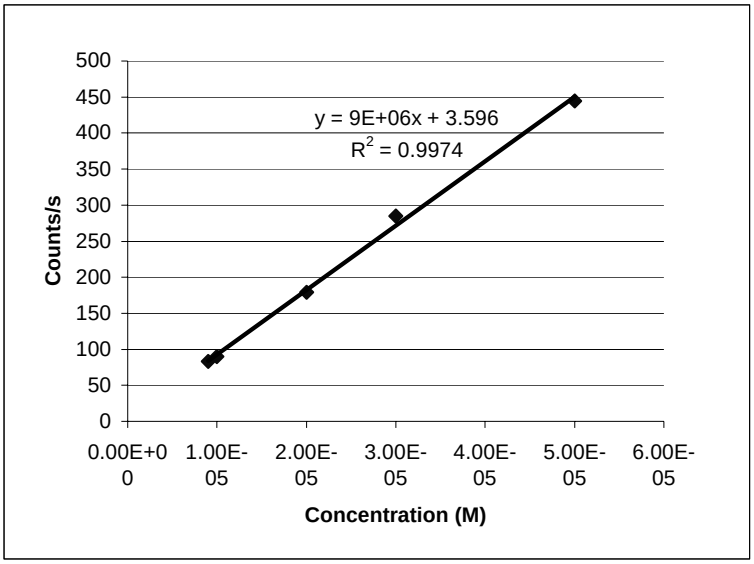

Figure 2-10. Calibration curve for tyrosine under pumped flow conditions. A detection limit of 2.0 μM was calculated at three times the standard deviation of the blank.

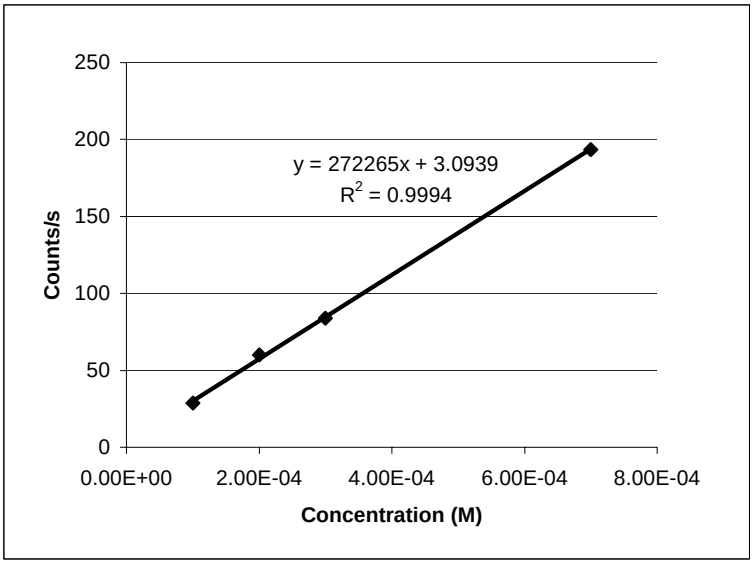

Figure 2-11. Calibration curve for phenylalanine under pumped flow conditions. A detection limit of 62 μM was calculated at three times the standard deviation of the blank.

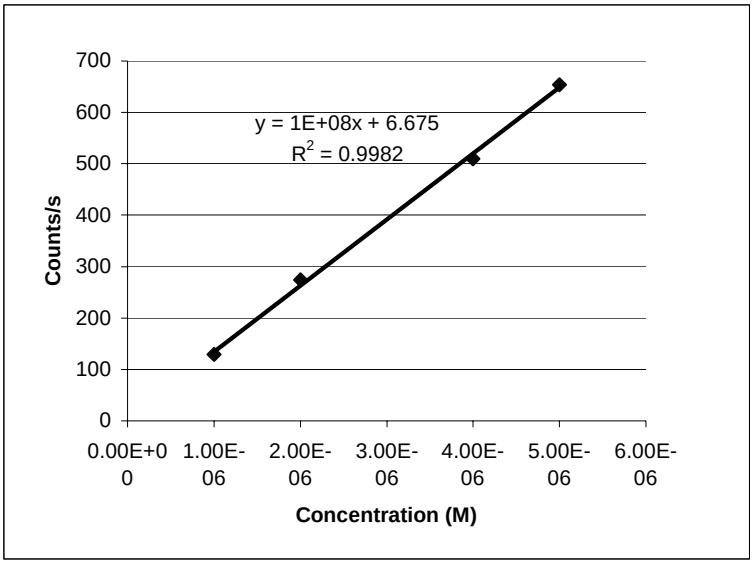

Figure 2-12. Calibration curve for BSA under pumped flow conditions. A detection limit of 0.13 μM was calculated at three times the standard deviation of the blank.

2.2.3 Characterization by Capillary Electrophoresis

To further characterize the suitability of the two-photon detector for μ-TAS, such as microchip CE and electric field gradient focusing (EFGF),[15] a simple, conventional capillary electrophoresis experiment was carried out.

A 3-mm patch of the polyimide coating was burned away from the center of a 40-cm piece of untreated, square fused silica capillary (50 μm square internal channel, Polymicro Technologies, Phoenix, AZ). The capillary was then held perpendicular to the excitation source and fixed to the base. To find the exact position of the capillary channel, a 0.1 M tryptophan solution was placed in the capillary and the capillary position was adjusted to maximize the fluorescence signal. After that, 1 M NaOH was manually pumped through the capillary using a syringe, followed by a buffer rinse. Then the ends of the capillary were immersed in the buffer reservoirs of a simple CE device shown schematically in Figure 2-13. Because the capillary was not treated inside, the electroosmotic flow (EOF) carried the analyte from the anode to cathode past the detection window. All samples used in the CE experiment were the same as in the flow cell experiment except that the buffer was changed from 10 mM pH 7 phosphate buffer to 100 mM pH 8.7 borate buffer. The borate buffer was made from boric acid powder (Fisher Scientific, Fair Lawn, NJ) and sodium hydroxide pellets (EMD, Gibbstown, NJ) dissolved in Millipore water.

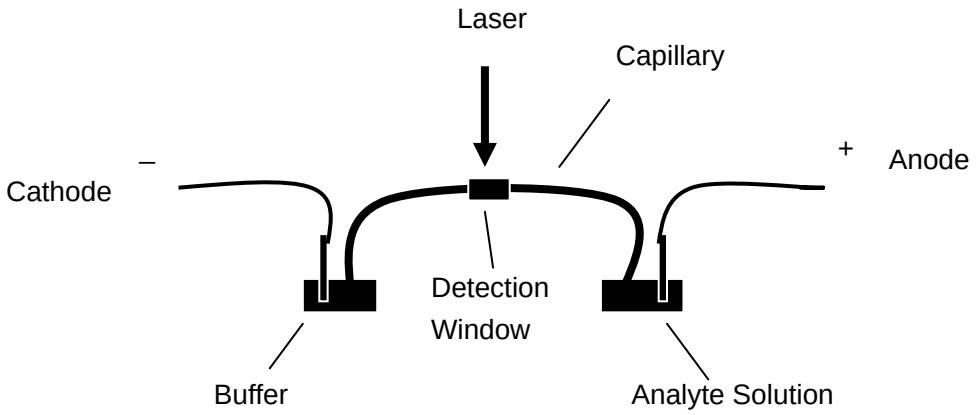

Figure 2-13. Schematic of the CE experiment.

First, the detection limit of tryptophan was measured under CE conditions. A series of tryptophan solutions with concentrations mentioned in Section 2.2.2 were placed in the analyte solution reservoir shown in Figure 2-13 in the order from lowest concentration to highest. Between each sample, the capillary was rinsed with pH 8.7 borate buffer. The tryptophan samples were injected for 2 s at 10 kV, and the inlet end of the capillary was transferred to the buffer reservoir. Finally, an operating voltage of 10 kV was applied to the electrodes for CE. Under EOF, analytes were carried by the buffer through the detection window and past the laser excitation source to give TPE fluorescence. The fluorescence signal was detected by a photon counter. Figure 2-14 shows an example of an electropherogram of 30 μM tryptophan.

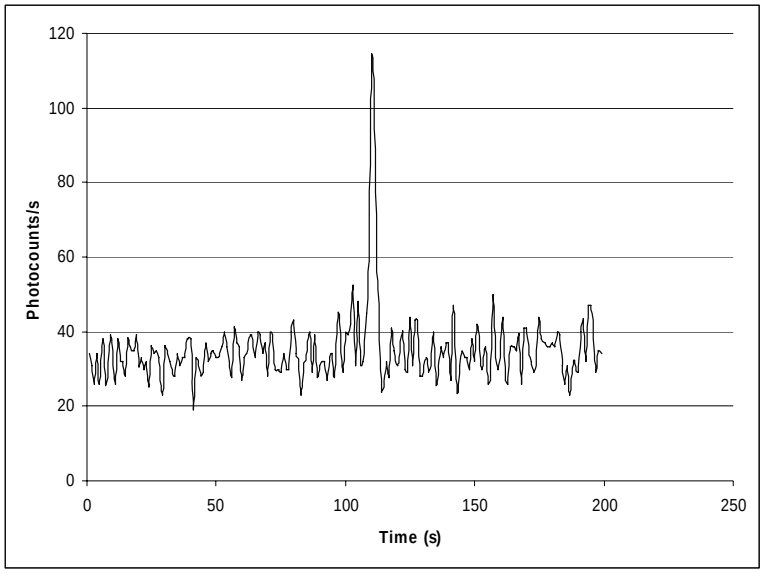

Figure 2-14. CE peak resulting from a 2 s injection of 30 μM tryptophan into a square capillary. Conditions: 10 kV separation voltage, 100 mM pH 8.7 borate buffer.

The detection limit of tryptophan in CE was determined by taking the peak values of each sample. These values were plotted against the corresponding concentration in Excel to form a calibration curve. The detection limit was calculated in the same way as that determined in the flow cell experiments. Figure 2-15 shows the calibration curve of tryptophan and the calculated detection limit of 5.8 μM.

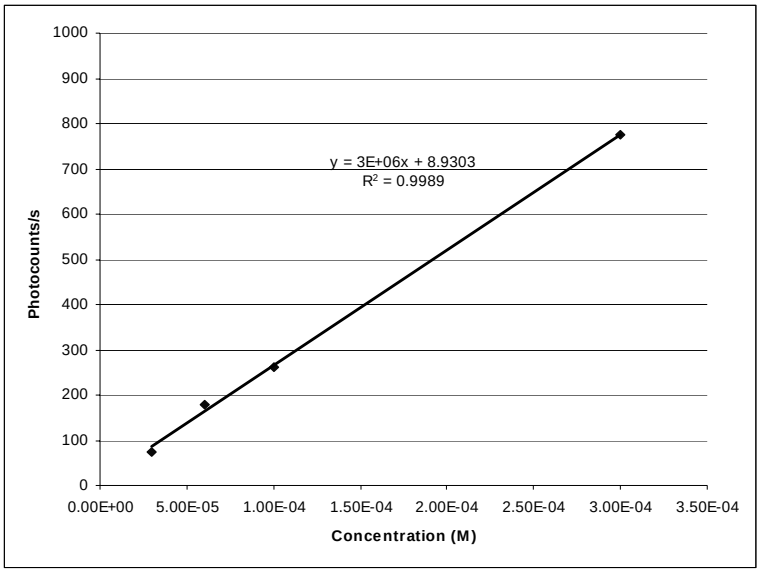

Figure 2-15. Calibration curve for tryptophan in CE. A detection limit of 5.8 μM was calculated at three times the standard deviation of the blank.

Finally, to demonstrate the applicability of this CE-TPE fluorescence system to a real sample, a mixture of aromatic amino acids was injected into the capillary. Figure 2-16 shows the separated peaks of 1 mM tryptophan and 3 mM tyrosine. The peaks were identified by spiking the sample with individual compounds.

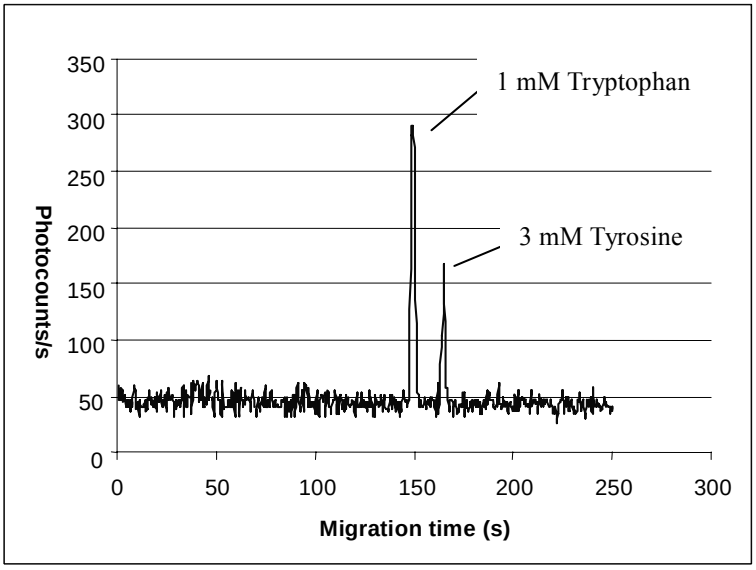

Figure 2-16. Electrophoregram of a sample mixture containing 1 mM tryptophan and 3 mM tyrosine. Conditions: 10 kV separation voltage, 100 mM pH 8.7 borate buffer, 0.5 s photon counter integration time.

2.3 Discussion

Our detector included a compact diode pumped solid state microchip laser, which used a saturable absorber embedded in the laser medium, thereby avoiding the costly and complicated use of electronics to drive traditional Q-switched lasers. The output of the laser was a train of 0.5 ns pulses with 29.3 mW average power at a repetition rate of 6.56 kHz, which can be translated into 8.9 kW peak power.

It is well known that in SPE, fluorescence emission is proportional to the excitation intensity. In contrast, in TPE, the emission intensity depends on the square of the incident light intensity.[4] Fisher[16] *et al.* further pointed out that two-photon fluorescence was proportional to the product of the average and peak powers of the laser, while SPE fluorescence was proportional only to the average power. According to $P_{peak}=P_{ave}/D$, where D is the duty cycle of the laser, and P_{peak}, P_{ave} are the peak and average powers of the laser, respectively, the laser's peak power depends on its duty cycle D, which is defined as the product of the laser pulse width and its repetition rate. Adoption of a high repetition rate laser with ultra short pulse width increases TPE fluorescence emission. Lippitz[10] used a 180 fs pulsed laser at a repetition rate of 76 MHz to achieve single molecule detection. The Webb[17] group was able to image TPE fluorescence from living cells by using a 100 fs pulsed dye laser at a repetition rate of about 80 MHz. We used a microchip laser producing only 0.5 ns pulses at a repetition rate of about 7 kHz. The relatively low repetition rate and wide pulses of the laser contribute to the relatively high detection limits obtained in our research.

For the three amino acids, tryptophan, tyrosine, and phenylalanine, SPE absorption maxima are at 278 nm, 275 nm, and 258 nm, respectively. [4] However, their two-photon excitation (TPE) maxima are not simply at twice the wavelengths of the SPEs. Rehms and Callis[18] studied TPE spectra of the three amino acids and compared them to that of SPE (shown in Figures 2-17, 2-18, 2-19, from Ref. 17). They pointed out that the TPEs of tyrosine and phenylalanine were blue-shifted relative to their SPEs because of the strong vibrationally induced component in TPE, which had much higher inducing mode frequency. However, for tryptophan, the induced component might behave much the same in SPE as in TPE. From Figures 2-17 to 2-19, tryptophan, tyrosine and phenylalanine have TPE maxima at 550 nm, 520 nm and 500 nm, respectively. So, the usage of a 532 nm YAG laser can efficiently excite the TPEs of tryptophan and tyrosine, but not phenylalanine.

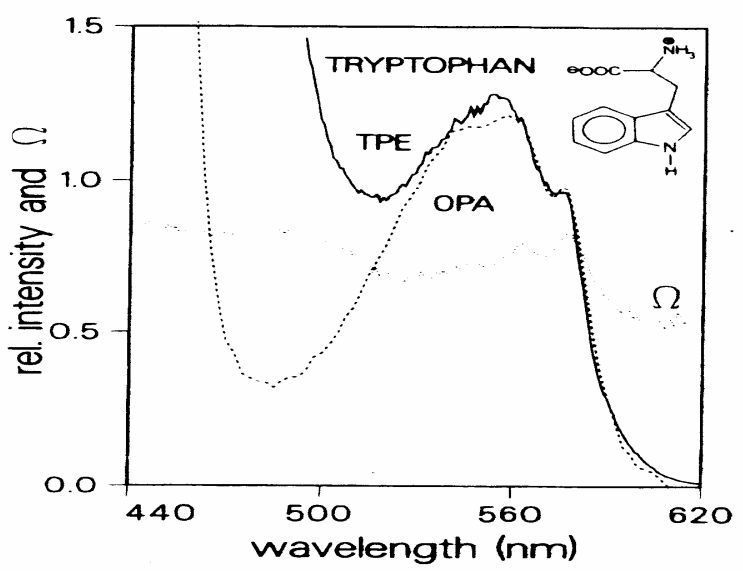

Figure 2-17. TPE and SPE (named as OPA in the figure) spectra for tryptophan. SPE is for wavelength at half the abscissa value [reprinted from Ref. 18, Copyright (1993), with permission from Elsevier].

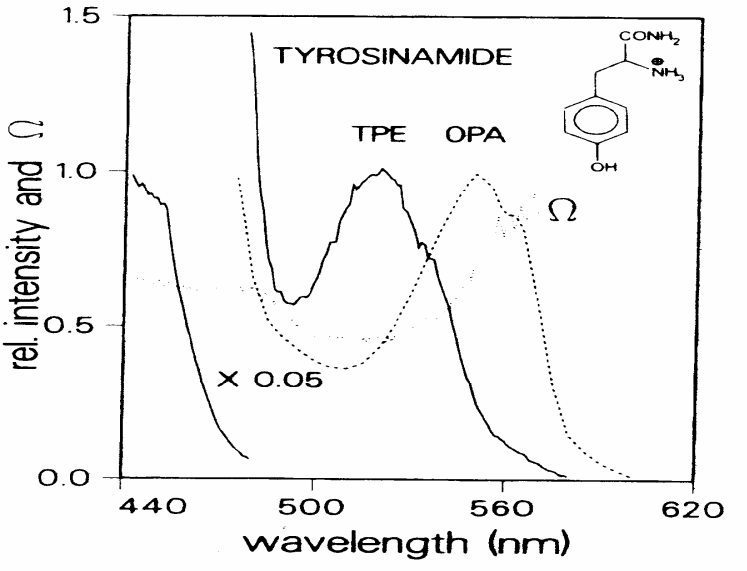

Figure 2-18. TPE and SPE (named as OPA in the figure) spectra for tyrosine (amide). SPE is for wavelength at half the abscissa value [reprinted from Ref. 18, Copyright (1993), with permission from Elsevier].

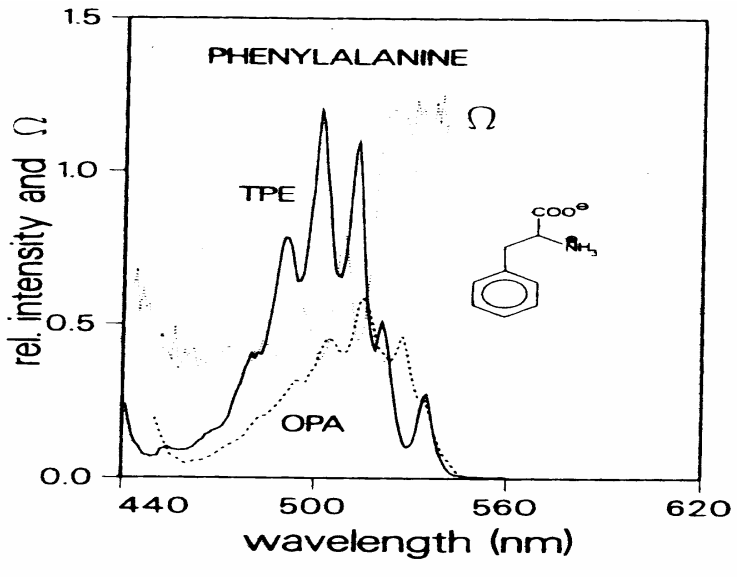

Figure 2-19. TPE and SPE (named as OPA in the figure) spectra for phenylalanine. SPE is for wavelength at half the abscissa value [reprinted from Ref. 18, Copyright (1993), with permission from Elsevier].

One of the characteristics of fluorescence is that the emission spectra are typically independent of the excitation wavelengths.[4] When it applies to TPE, the emission spectra of the same molecule should be the same as that of SPE. However, through the work of Xu *et al.*,[19] it was shown that, when excited at 532 nm, the two-photon fluorescence spectrum of tryptophan had a red shift of about 20 nm relative to its single-photon fluorescence at 348 nm. The red shift was 10 nm for tyrosine with single-photon fluorescence occurring at 303 nm. Although not studied for the case of phenylalanine, it could be inferred that the two-photon fluorescence of phenylalanine was somewhere close to its single-photon fluorescence at 282 nm. The mechanisms causing the red shift are not yet understood. The wavelength shifts can be used to explain the detection limit results of the three amino acids obtained in early experiments. Figure 2-20 shows the

transmission curve for the UG-11 filter, which transmits fluorescence but absorbs visible radiation. It is obvious that the UG-11 filter has poor transmission around 280 nm, so only a fraction of the phenylalanine fluorescence emission would be transmitted and detected by the PMT. Furthermore, the quantum yield of phenylalanine, 0.04, is lower than that of tryptophan, 0.20, and tyrosine, 0.21, in water at room temperature.[20] Given these factors, combined with the poor excitation efficiency mentioned in the above paragraph, it is not surprising that phenylalanine has a relatively higher detection limit than tryptophan and tyrosine.

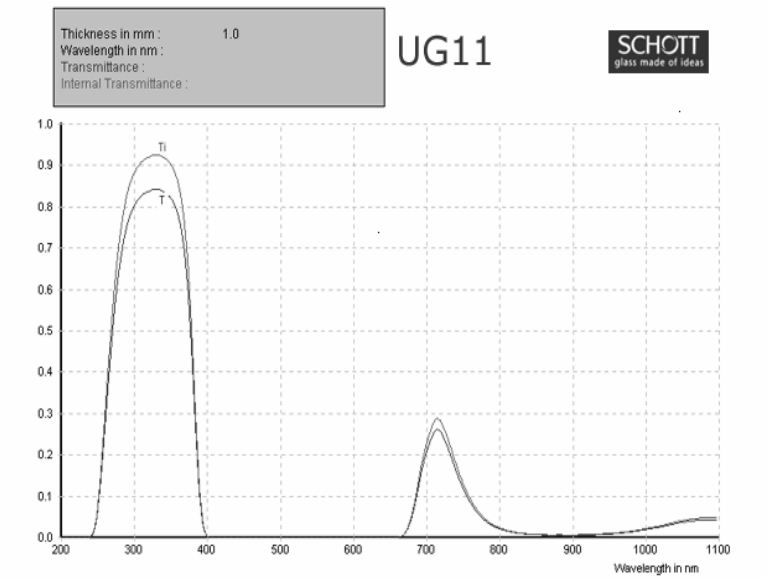

Figure 2-20. Transmission curve for a colored UG-11 filter (from Ref. 21)

Comparing the detection limits measured under static and pumped flow, it was found that detection limits are improved by a factor of 2.2, 4.2, 1.4, and 1.8 for tryptophan, tyrosine, phenylalanine, and BSA, respectively, in pumped flow compared to static flow. Lippitz *et al.* [10] studied two-photon fluorescence quantum efficiency and

photobleaching quantum efficiency of unbound tryptophan in solution, tryptophan in hemobyanin, and tryptophan in avidin bound to latex spheres. They found that free tryptophans in buffer solution had the highest photobleaching quantum efficiency and emitted an average of 2 photons per tryptophan before photobleaching. This number increased to 180 photons per tryptophan residue in avidin-coated spheres, which had 340 tryptophans per sphere. From the Lippitz experiments, it is clear that the signal depends not only on the number of tryptophan residues in the detection volume, but also on the molecular environment in which they are found. To minimize the impact of photobleaching, we flowed the sample at a rate that guaranteed a fresh volume for each laser shot. Because of the effect of photobleaching, the relatively low repetition rate of the microchip laser is well suited for protein detection.

Aromatic amino acids can be found in biological molecules and exhibit native fluorescence. Among the three amino acids studied here, tryptophan has the longest absorption wavelength. Because of its long absorption wavelength, energy absorbed by phenylalanine and tyrosine residues is often transferred to tryptophan residues in the same protein. In fact, energy transfer has been repeatedly observed in proteins which contain both tyrosine (or phenylalanine) and tryptophan, which is one reason for the minor contribution of phenylalanine and tyrosine to fluorescence emission.[4] For example, the fluorescence quantum yield of tyrosine is about 0.02 in serum albumin and egg albumin, only 10% of the value in free tyrosine.[20,22] However, the corresponding yields for tryptophan vary in different proteins from about 0.05 (bovine γ-globulin) to 0.48

(BSA).[20] The phenomenon that the quantum yield of tryptophan in BSA is larger than the value of 0.20 in free tryptophan is a good proof of energy transfer. Since the higher quantum yield proteins facilitate fluorescence observation, we chose BSA as a test protein in our research.

To test the sensitivity of the detector toward microscale analysis, CE was performed in a square capillary having 50-μm i.d. Square capillaries are superior to round capillaries for TPE. Overway and Lytle[23] experimented with these two kinds of capillaries and found that the phenomenon of beam astigmatism was severe in round capillaries. The beam astigmatism was caused by focal differences between rays in a plane longitudinal to the capillary and rays in a plane transverse to the capillary. The square capillary overcame this problem by providing a larger and flatter effective internal surface area.

In theory, the intensity of two-photon excited fluorescence is inversely proportional to the beam diameter. For a tightly focused laser, this property results in emission originating from a region near the focal point. Thus, detection limits obtained with microscopic sample volumes (the capillary) should be nearly the same as those observed with macroscopic volumes (the flow cell).[23] However, the detection limit of tryptophan was 5.8 μM in the capillary, about 12 times higher than in the 1.0-mm quartz flow cell. The discrepancy between the theoretical and the practical is mainly due to the following two factors. First, the optical quality of the capillary is poorer than that of the flow cell, which resulted in a distorted shaped laser focus inside the capillary. Second, the analyte solution injected into the capillary was diluted because of the phenomenon of

diffusional broadening, which raised the detection limit of tryptophan.

The careful reader will have noticed that the signals in Figure 2-16 do not scale linearly with the signals for lower concentrations in Figure 2-14. The concentrations injected for Figure 2-16 are outside the linear dynamic range for these analytes,[12] so the low signals relative to a linear response are to be expected.

2.4 References

1. Lu, H.P., Xun, L.Y., Xie, X.S. *Science* **1998**, *282*, 1877-1882
2. Haupts, U., Maiti, S., Schwille, P., Webb, W.W. *Proc. Natl. Acad. Sci. USA* **1998**, *95*, 13573-13578
3. Schwille, P., Haupts, U., Maiti, S., Webb, W.W. *Biophys. J.* **1999**, *77*, 2251-2265
4. Lakowicz, J. *Principles of fluorescence spectroscopy* Kluwer Academic/Plenum Publishers **1999** 2nd ed.
5. Peck, K., Stryer, L., Glazer, A., Mathies, R. *Proc. Nat. Acad. Sci.* **1989**, *86*, 4087-4091
6. Dickson, R., Cubitt, A., Tsien, R., Moerner, W. *Nature (London)* **1997**, *388***,** 355-358
7. Wennmalm, S., Blom, H., Wallerman, L., Rigler, R. *Biol. Chem.* **2001**, *382*, 393-397
8. Diaspro, A., Robello, M. *J. Photochem. Photobiol. B: Biol* **2000**, *55*, 1-8
9. Okerberg, E., Shear, J. *Anal. Chem.* **2001**, *73*, 1610-1613
10. Lippitz, M., Erker, W., Decker, H., Holde, K., Basche, T. *Proc. Nat. Acad. Sci.* **2002,** *99***,** 2772-2777

11. Paul, U. http://contentdm.lib.byu.edu/ETD/image/etd416.pdf

12. Paul, U., Li, L., Lee, M., Farnsworth, P. *Anal. Chem.* **2005,** *77,* 3690-3693

13. Zugel, S., Lytle, F. *Appl. Spectrosc.* **2000**, *54*,1490-1494

14. http://www.friedli.com/research/PhD/chapter5a.html#amino Accessed Nov. 21, 2005

15. Humble, P., Kelly, R. Woolley, A. Tolley, H. Lee, M. *Anal. Chem.* **2004**, *76*, 5641-5648

16. Fisher, W., Lytle, F. *Anal. Chem.* **1993**, *65*, 631-635

17. Denk, W., Strickler, J. H., Webb, W. W. *Science* **1990**, *248,* 73-76

18. Rehms, A., Callis, P. *Chem. Phys. Lett.* **1993**, *208*, 276-282

19. Xu, Y., Zhang, J., Deng, Y., Hui, L., Jiang, S., Lian, S. *J. Photochem. Photobiol. B: Biol* **1987**, *1*, 223-227

20. Truong, T., Bersohn, R., Brumer, P., Luk, C., Tao, T. *J. Biol. Chem.* **1967**, *242*, 2979-2985

21. http://www.optical-filgers.com Accessed November 10, 2005

22. Teale, F. *Biochem. J.* **1960**, *76*, 381

23. Overway, K., Lytle, F. *Appl. Spectrosc*. **1998**, *52***,** 928-932

Chapter 3

Two-Photon Microscope Setup and Characterization

3.1 Introduction

As mentioned in Chapter 2 in this thesis, the ultimate goal of building a TPE fluorescence detector is to work with microchip separations of proteins. The two-photon prototype detector described in Chapter 2 has proven effective and sensitive toward native fluorescence detection of biomolecules. The success of the prototype detector demonstrated that I had gained sufficient practical experience and skill to build a protein detector based on two-photon excitation (TPE), a quickly growing technique.[1] However, because the prototype detector had no provision for directly viewing the location illuminated by the laser, it was very difficult to align it with the microscopic features of a microchip separation device. A more precise way to do laser focusing inside microchip channels was needed. A trinocular two-photon microscope was the best solution for the problem.

Unfortunately, there are very few commercially available two-photon microscope systems, and the available systems cost typically over $500 K.[2] In addition to the limited availability and high cost, such systems are large, delicate and need professional operators. In my work, the purpose of constructing a two-photon microscope was to enable precise laser focusing. To meet my needs, I chose to adapt a commercially available conventional fluorescence microscope for two-photon excitation. Adapting a

commercial microscope gave the maximum flexibility to choose all the components, such as the microscope, optics, and laser, and allowed me to design the system to the specific requirements of my application.[3]

Many groups have successfully adapted an existing microscope system for two-photon excitation. The Fraser group[4] converted a Molecular Dynamics Sarastro 2000 confocal microscope by introducing a pulsed infrared Ti/Sapphire laser, which usually costs ~$135,000. They replaced broad-spectrum (infrared and visible) mirrors and installed a beam-splitter to separate the infrared excitation from the visible fluorescence. The Parker group[2] constructed a custom two-photon system for video-rate Ca^{2+} imaging. Derived from their previous design of a confocal microscope, the major change was the introduction of a femtosecond pulsed Ti/Sapphire laser. The total construction cost they reported was about $175,000, of which over $100,000 was accounted for by the laser. In fact, the mode-locked Ti/Sapphire laser has become the most versatile pulsed infrared laser for two-photon microscopy. The features of the laser include high average power, high repetition rate and short pulse width. All of these are critical for efficient two-photon excitation.[1] However, these laser systems are bulky and expensive, and need extensive water cooling and complicated electrical supplies.[3,5] Even the more compact versions of the Ti/Sapphire laser, which do not need dedicated water cooling and are easy to install, still have the disadvantage of being priced similar to more powerful and flexible Ti/Sappire units although the compact versions are less powerful and not tunable.[2,3]

To circumvent these limitations, I used a compact solid state microchip nanolaser

in the custom-made two-photon microscope, which was a major change to the original microscope. This laser had much smaller size (145 mm×35 mm×30 mm) compared to Ti/Sapphire lasers and cost only ~$6,000. Other than a heat sink attached to the base plate for thermal dissipation, this laser did not need any extra cooling system. The heat generated during more than 4 h of laser operation could be effectively dissipated by the heat sink in a well-ventilated lab. Even an untrained person could use this laser because of its easy turnkey operation. Other changes made to the original microscope included the introduction of a beam expander, a two-photon cube with dichroic mirror and filters, a tube lens, and a PMT as detector. The total construction cost was estimated at no more than $10,000.

In this chapter, I present details of the construction of a two-photon microscope, considerations that led to the final design, and optimization of the microscope beam path. Then I show preliminary measurements of tryptophan for characterizing the instrument. Examples of the microchip separations will be discussed in Chapter 4.

3.2 Microscope Construction

3.2.1 Overview

Figure 3-1 shows a schematic diagram of the two-photon microscope, and Figure 3-2 shows a photograph of the instrument. Key components were the compact solid-state Nd/YAG laser generating sub-nanosecond pulses of green light, an upright Olympus BX60M microscope, and a photomultiplier tube (PMT) detector mounted on

the microscope trinocular head. In addition, the microscope was equipped with beam expanders, filters, a dichroic mirror, and tube lens.

The laser beam was first passed through a 15× beam expander. A CG-495 filter removed the low level of 355 nm background from the laser. After that, the laser was directed to a dichroic mirror and reflected downward toward the microscope objective. The microscope objective focused the collimated laser beam to a 1-μm spot. Two-photon fluorescence generated from the samples was collected by the same objective, and transmitted through the dichroic mirror and a UG-11 filter, which removed any scattered laser light and transmitted the UV fluorescence. The fluorescence emission was finally focused by an air-spaced achromatic doublet through an aperture onto a PMT. The signal detected by the PMT was first amplified, and then sent to a gated photon counter. A Labview virtual instrument was used to acquire data.

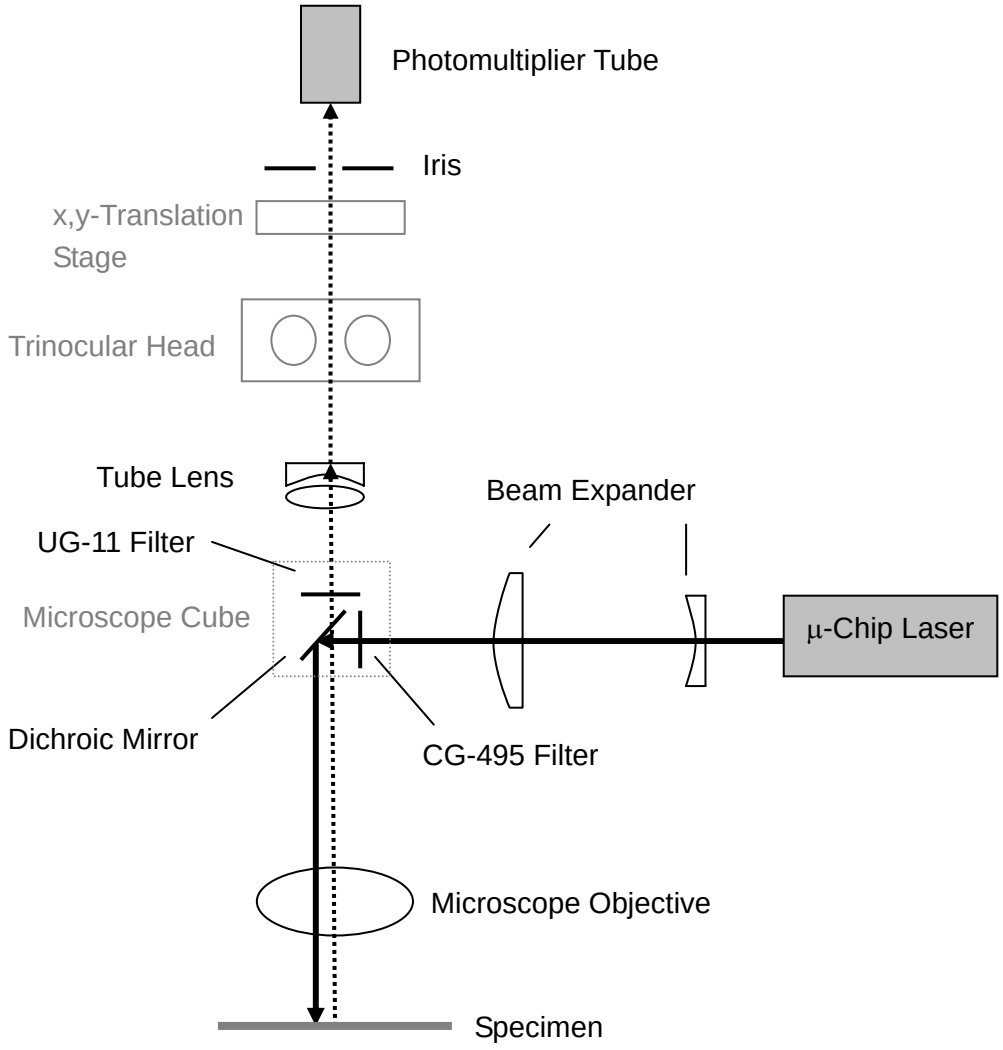

Figure 3-1. Schematic diagram of optical components of the custom two-photon microscope viewed from the front. Solid lines represent laser excitation and dashed lines represent two-photon fluorescence.

Figure 3-2. Photograph of the two-photon microscope system.

3.2.2 Laser

A pulsed diode-pumped solid state microchip nanolaser (JDS Uniphase, San Jose, CA) was used as the excitation source in the two-photon microscope. This Nd/YAG laser was frequency-doubled, producing radiation at 532 nm. It had an average power of 23.3 mW, a pulse width of 0.6 ns, a pulse repetition rate of 7.75 kHz, and calculated peak power of 5 kW if assuming a rectangular pulse shape. Compared to the large and expensive Ti/Sapphire lasers, this laser, based on the new diode-pumped solid-state technology, has the advantages of lower price and smaller size.[3]

Since the first introduction of two-photon excitation in 1931,[6] multiphoton excitation and fluorescence has been used in molecular spectroscopy of various materials.[7,8] One of its significant applications is in the biological fields. The Webb group first demonstrated a two-photon laser scanning microscope (TPLSM) in 1990 to obtain fluorescence images of living cells.[9] After that, TPLSM has become a powerful technique for three-dimensionally resolved fluorescence imaging of biological samples.[10,11] The fast development of TPLSM is mostly dependent on the availability of mode-locked femtosecond lasers.[7,12] Among these, the Ti/Sapphire laser is the most popular. Not only can it produce femtosecond pulses, but also an average power as high as 800 mW.[1] The high power of the laser is believed to be critical for imaging biological samples, especially dimmer samples in TPLSM.[3] Most Ti/Sapphire lasers also have tunable outputs from 650 to 1050 nm. This property expands the application of TPLSM because different fluorophores can be excited over a wide range of wavelengths.[13]

However, in my research, the goal of constructing a two-photon microscope was not for biological sample imaging but for solving the problem of precise laser focusing into microchannels for protein detection. Expensive, bulky, and high powered femtosecond lasers were neither practical nor necessary for this microscope. The solid-state microchip laser I am currently using was well suited for my research purposes with compact size and low cost. The modest power output was enough for two-photon excitation without causing serious photobleaching to the samples. Since I aim to detect proteins based on their native fluorescence which can be excited at 275 nm,[14] the single wavelength at 532 nm of this laser can be applied to all analytes of interest in this research.

3.2.3 Beam Expander

A beam expander was introduced inside the collector lens unit of the microscope. The beam expander consisted of a plano-convex lens (PLCX-25.4-77.3-UV-532, purchased from CVI, Albuquerque, NM) and a plano-concave lens (PLCC F-10 Dia 5, Melles Griot, Rochester, NY). Both of them were anti-reflection coated at 532 nm. The manufacturer's nominal focal lengths for these two lenses were 150 mm and 10 mm, respectively, giving the beam expander a magnification of 15. The original laser beam diameter was 0.2 mm. After passing through the beam expander, the laser beam spot had a diameter of 3 mm. Because the laser was slightly divergent, the actual laser beam, measured right after the beam expander, was ~ 4 mm in diameter.

In many quantitative measurements, such as multiphoton photobleaching recovery measurements,[15] and focal uncaging or photochemistry,[16,17] it is important to have the beam overfill the back aperture of the objective in order to improve the spatial resolution.[3] Although I made no attempt to investigate spatial resolution in this research, the laser beam expansion was important not only because it reduced the beam energy when the laser hit the optics but also produced a collimated beam.[18]

3.2.4 Microscope cubes

Two microscope cubes were placed inside the universal cube housing of the microscope. One was for the two-photon fluorescence experiment and the other was to allow the operator to view the region being probed (called the "observation cube"). The two-photon fluorescence cube included a dichroic mirror, a long pass filter, and a UG-11 filter. The long pass filter (W2-CG-GG-495-1.00-2.5-532, CVI, Albuquerque, NM) removed the third harmonic at 355 nm of the laser (the detailed discussion of 355 nm background can be found in Chapter 2). The dichroic mirror (SWP-45-RS532-TU280-400-RW-38.0-26.0-1.0-UV, CVI, Albuquerque, NM), located right behind the long pass filter, reflected more than 99.5% of 532 nm laser radiation downward toward the microscope objective. UV fluorescence emission, collected by the same objective, passed through the dichroic mirror with 85% efficiency, and then through a UG-11 filter (CG-UG-11-1.00-2, CVI, Albuquerque, NM), which removed scattered laser light while transmitting fluorescence, a tube lens, and an iris, and finally hit a PMT. Because the UG-

11 filter also had a transmission window in the near IR that transmitted unwanted long wavelength light, the PMT chosen in this microscope had no response to near IR light.

The two-photon fluorescence and observation cubes could be easily switched to the working position by rotating the turret. Introduction of an observation cube allowed viewing of samples through eyepieces of the microscope. With the two-photon cube in place, the sample could not be seen because the UG-11 filter prevented any visible light from reaching the eyepieces and other downstream optics. Inside the observation cube were a neutral density filter (FBR-ND30, Newport, Irvine, CA) and a dichroic mirror (FF555-Di02-25×36, Semrock, Rochester, NY). The neutral density filter attenuated the laser beam by 1,000 times before it hit the dichroic mirror. This beam attenuation was necessary to prevent dangerous levels of laser light from reaching the operator's eyes. The dichroic mirror was designed to reflect light from 493 nm to 548 nm (the 532 nm laser fell in this range) and transmit from 562 nm to 745 nm (any fluorophores having fluorescence emission wavelengths in this range were useable, for example, rhodamine B).

3.2.5 Microscope objectives

The microscope objective focused the collimated laser light, which was reflected from the dichroic mirror, to a 1-μm spot. The excited fluorescence was then collected by the same objective, transmitted through the dichroic mirror, a UG-11 filter and a tube lens before it was detected by a PMT.

Two microscope objectives were tested. One was a UV achromatic objective used in the prototype two-photon detector described in Chapter 2 and the other was a reflective objective (model No. 13596 36×, ThermoOriel, CT). The reflective objective was usable from 200 nm to 20 μm and had an entrance aperture of 5.3 mm. As discussed previously in the section on the beam expander, the laser beam had a practical diameter of ~4 mm after expansion, which filled the reflective objective but not the UV achromatic objective, which had an entrance aperture of 8 mm. It should also be noted that, through the discussion in Chapter 2, because the laser radiation was not in the achromatic design range (194 nm to 450 nm) of the UV achromatic objective, the two-photon fluorescence was not collimated after collection by this objective.

3.2.6 Tube lens

A UV-visible achromatic lens (LAU-25-200-UVB, focal length 200 mm, OFR, Caldwell, NJ), fitted inside a custom machined, black anodized, aluminum tube, was mounted between the cube housing and the trinocular head of the microscope. This air-spaced doublet was anti-reflection coated especially for this research from 240 nm to 360 nm. The fluorescence beam, although not perfectly collimated by the UV achromatic objective, was focused into a small spot by the tube lens before hitting the PMT.

3.2.7 PMT

An iris was placed at the focal point of the tube lens to reduce background light

levels. The iris blocked some reflections from optic surfaces, scattering from the walls of sample cells, and long wavelength (single-photon) fluorescence.

The PMT (H6780-03, Hamamatsu, Japan) used in this microscope was the same as was used in the prototype detector. It was a self-contained assembly with a head-on PMT and a high voltage power supply, which avoided the necessity for the user to deal with high voltages. The spectral response range for this PMT was from 185 nm to 650 nm, compatible with the IR transmission property of the UG-11 filter.

The iris and the PMT were mounted on an x-y translation stage. This allowed small scale adjustments of the x-y position of the iris to perfectly match fluorescence emission and direct it onto the active area of the PMT. The x-y translation stage was mounted on an externally threaded portion of a lens tube. By threading the translation stage along threads of that tube, the vertical distance could be adjusted to match the appropriate UV fluorescence focus of the tube lens.

When in use, the PMT was highly susceptible to stray room light. To circumvent this problem, it was necessary to tape the iris with black tape and turn off the room light when the PMT was on.

3.2.8 Beam Path Alignment

The laser was mounted on a 5-axis lens positioner (model LP-1A, Newport, CA), which allowed five degrees of freedom to accurately align the laser beam to the microscope optics. It was necessary to adjust the separation between the two lenses in the

beam expander to produce a collimated beam. This was achieved by fitting the plano-concave lens inside a short tube which was threaded into the outside end of the collector lens unit of the microscope. The appropriate distance was decided by threading the short tube in and out of the collector lens unit and picking the distance at which the expanded beam was collimated.

The fluorescence collected by the objective passed through the dichroic mirror, the UG-11 filter, the tube lens, and the iris to the PMT. Alignment of this emission beam path could be easily done by threading the whole piece of the x-y translation stage and iris along an externally threaded tube (like mentioned in section 2.2.7), which changed the distance from the iris to the tube lens. By tuning the micrometer translation stage on which the iris and the PMT were mounted, the emission light could be directed through the iris to the PMT.

3.3 System Characterization and Results

3.3.1 Iris Aperture Size Determination

At first, the iris aperture was left at 1 mm diameter and the sensitivity of the microscope was tested with a 0.1 mM tryptophan solution. The fluorescence signal was found to be much lower than that obtained by the prototype detector under the same conditions. However, the signal increased as the iris was opened. Figure 3-3 shows the signal variation with change in the aperture size. Both 70 μM tryptophan solution and 10 mM phosphate buffer were tested. The triangular dots represent the results of subtracting

the buffer signal from the analyte signal. The photon count value for each point was the average of 50 data points.

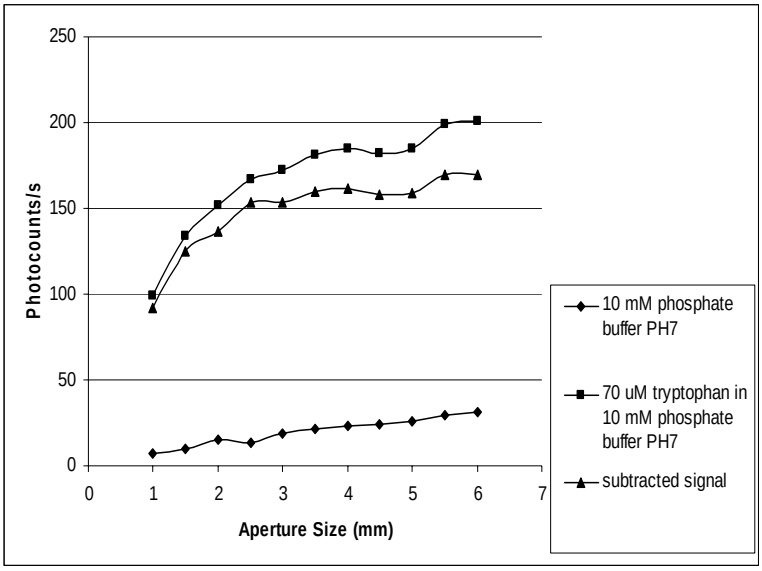

Figure 3-3. Two-photon fluorescence signal of 70 μM tryptophan for different aperture sizes.

In Figure 3-3, the signal (represented by squares) increased dramatically until the iris reached 2.5 mm. After 2.5 mm, it increased slowly. The blank (represented by diamonds) also increased up to 2 mm. Then it decreased at 2.5 mm. For the subtracted signal (represented by triangles), it showed an increasing trend before 2.5 mm and this trend became less significant after that. Because the 2.5 mm aperture gave the highest signal-to-noise ratio, the iris was set at that value for the two-photon microscope.

3.3.2 Detection Limits of Tryptophan

To determine the sensitivity of the two-photon microscope detector, calibration curves of tryptophan were obtained by using both UV achromatic and reflective objectives. Solutions ranging from 10 μM to 70 μM were prepared by diluting the stock solution of 1 mM tryptophan and pumping it through the 1-mm quartz flow cell. Two-photon fluorescence signals were recorded by the photon counter. Figures 3-4 and 3-5 show the calibration curves of tryptophan using UV achromatic and reflective objectives, respectively. The detection limits of tryptophan, calculated from the calibration curves, are 1.0 μM and 790 nM, respectively.

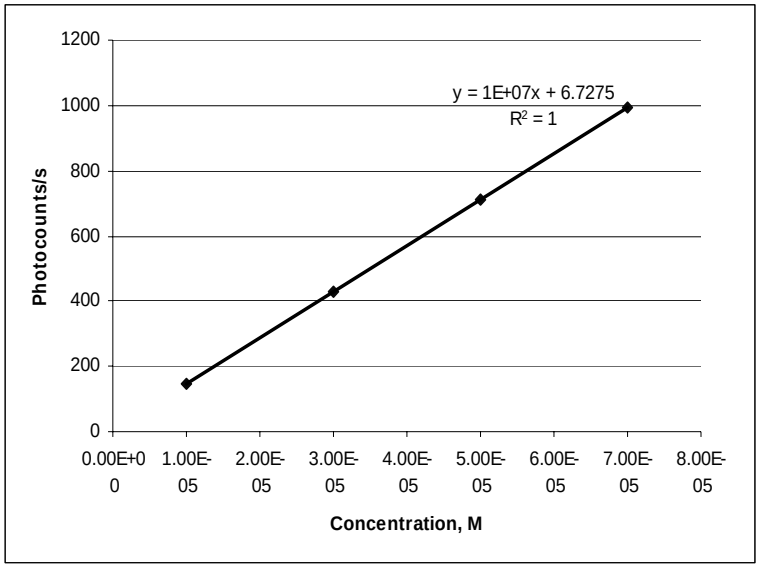

Figure 3-4. Calibration curve for tryptophan under pumped flow conditions using the UV achromatic objective. A detection limit of 1.0 μM was calculated at three times the standard deviation of the blank.

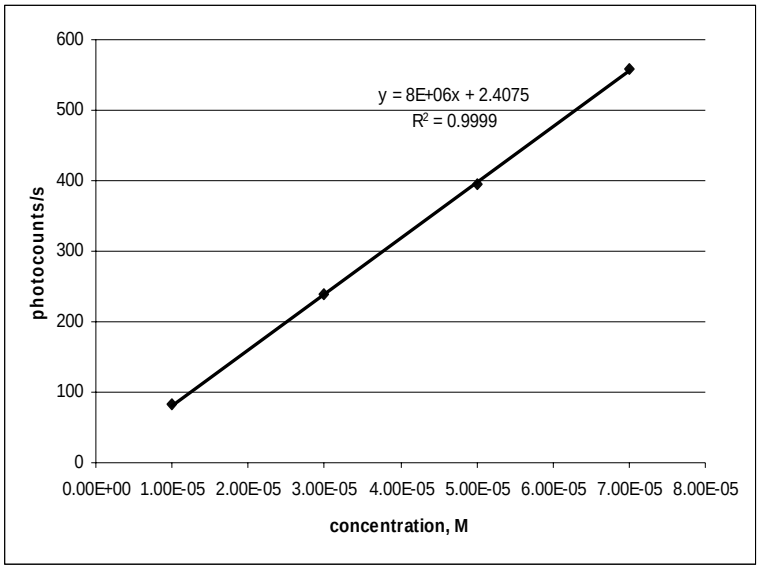

Figure 3-5. Calibration curve for tryptophan under pumped flow conditions using the reflective objective. A detection limit of 790 nM was calculated at three times the standard deviation of the blank.

3.4 Discussion

The purpose of constructing a two-photon microscope was to have a precise way to focus the laser into a microchannel. The trinocular observation tube on the commercial microscope allowed the operator to see the focal point. The most significant change in the microscope described in this chapter was the removal of a glass compensator from the trinocular tube. This glass compensator absorbed UV light. Without it, UV fluorescence emission passed to the PMT and was detected as a signal. Another change was the introduction of an observation filter cube. Because of the UG-11 filter in the two-photon cube, microscope illumination light wasn't transmitted to the trinocular observation tube to allow viewing. Adding a visible cube overcame this problem. This was especially important for the work done inside a microchannel described in the next chapter. All of the characterization work described in this chapter was done inside a 1 mm flow cell, so, the visible cube was not used.

Originally it was difficult to align the fluorescence beam path because of the absence of suitable light sources. The fluorescence generated by my experiment or emitted from a UV LED was too weak to see. Furthermore, the fluorescence involved in my research was around 350 nm which was not visible to the naked eye. UV operation made alignment difficult. Finally, I just used scattered laser light collected by the microscope objective to do this job. Not much difference between laser light and real fluorescence emission was expected since the tube lens, which focused collimated light into a spot, was UV-visible achromatic. It decreased the focusing differences in those two

cases to a minimum. It is worth noting that the UG-11 filter had to be taken out when performing the alignment.

Usually the confocal pinhole is not necessary in a TPE fluorescence setup. Because the TPE is made possible by simultaneous absorption of two photons, it happens predominantly in the highly defined focal volume by a high numerical aperture microscope objective. The high confinement of fluorescence excitation to the focal volume produces a confocal-like effect even without the necessity of a confocal pinhole.[19,20]

However, I kept the confocal pinhole in the microscope because I found that the two-photon fluorescence signal/noise increased with increasing the iris aperture (shown in Figure 3-3), which indicated that the fluorescence focusing spot I obtained with the microscope setup had a relatively large size. This may be due to the imperfect performance of the UV achromatic microscope objective, since the laser wavelength was not within the designed wavelengths of the objective. As a result, the fluorescence may not be perfectly focused into a spot by the tube lens.

Nowadays, two-photon microscopes are widely used for three-dimensional imaging of biological systems.[5,9,21] Confocal pinholes are usually kept in order to obtain a better spatial resolution.[19] It has been reported that when a pinhole is necessary, the axial resolution can be improved by approximately 40%.[22] Although I am not doing any imaging, a pinhole is useful for the two-photon microscope system.

3.5 References

1. Diaspro, A.; Corosu, M.; Ramoino, P.; Robello, M. *Microsc. Res. Tech.* **1999**, *47*, 196-205
2. Nguyen, Q.; Callamaras, N.; Hsieh, C.; Parker, I. *Cell Calcium* **2001**, *30*, 383-393
3. Majewska, A.; Yiu, G.; Yuste, R. *Pflugers Arch – Eur. J. Physiol.* **2000**, *441*, 398-408
4. Potter, S.; Wang, C.; Garrity, P.; Fraser, S. *Gene* **1996**, *173*, 25-31
5. Potter, S. *Curr. Biol.* **1996**, *6*, 1595-1598
6. Göppert-Mayer, M. *Ann. Phys.* **1931**, *9*, 273-295
7. Xu, C.; Zipfel, W.; Shear, J.; Williams, R.; Webb, W. *Proc. Natl. Acad. Sci. USA* **1996**, *93*, 10763-10768
8. Shreve, A.; Trautmen, J.; Owens, T.; Albrecht, A. *Chem. Phys. Lett.* **1990**, *170*, 51-56
9. Denk, W.; Strickler, J.; Webb, W. *Science* **1990**, *248*, 73-76
10. Parker, I.; Choi, J.; Yao, Y. *Cell Calcium* **1995**, *20*, 105-121
11. Yuste, R.; Denk, W. *Nature (London)* **1995**, *375*, 682-684
12. Spence, D.; Kean, P.; Sibbett, W. *Opt. Lett.* **1991**, *16*, 42-44
13. Denk, W.; Piston, D.; Webb, W. *Handbook of Biological Confocal Microscopy* edited by Pawley JB. New York: Plenum, **1995**, pp. 445-458
14. Chang, H.; Yeung, E. *Anal. Chem.* **1993**, *65*, 2947-2951
15. Brown, E.; Wu, E.; Zipfel W.; Webb, W. *Biophys. J* **1999**, *77*, 2837-2849
16. Brown, E.; Shear, J.; Adams, S.; Tsien, R.; Webb, W. *Biophys. J* **1999**, *76*, 489-499
17. Denk, W. *Proc. Natl. Acad. Sci. USA* **1994**, *91*, 6629-6633

18. Paul, U.; Li, L.; Lee, M.; Farnsworth, P. *Anal. Chem.* **2005**, *77*, 3690-3693

19. Diaspro, A.; Robello, M. *J. Photochem. Photobiol. B:Biol.* **2000**, *55*, 1-8

20. Piston, D.; Kirby, M.; Cheng, H.; Lederer, W.; Webb, W. *Appl. Opt.* **1994**, *33*, 662-669

21. Piston, D. *Trends Cell Biol.* **1999**, *9*, 66-69

22. Gu, M.; Sheppard, C. *J. Mod. Opt.* **1993**, *40*, 2009-2024

Chapter 4

Design and Performance of Microchips Coupled with the Two-Photon Microscope

4.1 Introduction

Microchip based analytical devices have become more and more attractive in recent years since the first introduction of micro total analysis systems (μTAS).[1] Among various separation techniques performed on microchips, such as chromatography, electrophoresis and electrochromatography, capillary electrophoresis (CE) has become the most highly developed technique. Microchip CE has the advantages of rapid separation, small sample volumes, low reagent consumption and simple channel fabrication and operation.[2] It has been widely used to analyze various biologically important molecules, especially in the field of proteomics.[3]

While the advantages of microchip CE are highly dependent on its miniaturized size, this compact format also presents challenges for detection.[4] Conventional UV absorbance has an inherent problem of linear dependence on optical path length, which leads to poor sensitivity in small-scale microchips. Laser induced fluorescence (LIF) has become the most commonly used detection technique in microchip CE, not only because of its high sensitivity, [5] but also because it is easily coupled to the experimental system using an epi-fluorescence setup.[4] However, most analytes need to be labeled with a fluorescent tag before they can be excited by a visible laser (for example, a 488 nm laser).

This procedure makes the whole analysis more complex because tagging needs additional sample treatment and may affect the efficiency of separation.

Laser-induced two-photon excitation (TPE), described in previous chapters, is a good choice to excite the native fluorescence of samples with visible radiation without any extra labeling. The inherent nonlinear nature of TPE, different from the linear property of SPE, restricts the fluorescence to a very small volume defined by the diffraction-limited focusing of the objective.[6,7] This makes it a promising method for detection when using micro-scale devices. Although most biomolecules containing tryptophan, tyrosine, and phenylalanine can be excited by a UV laser (for example, a 266 nm laser) based on SPE, the adoption of a 532 nm green laser in TPE is more favorable since it eliminates the requirements of expensive UV lasers and UV transparent optics used in SPE.

Poly (methyl methacrylate) (PMMA) was considered to be the first choice of substrate for microchip devices in this research. Being one of the fastest growing polymer substrates used for microfluidic devices, PMMA not only has the common advantages of polymers, such as biocompatibility[8] and easy manipulation, but it is also less hydrophobic than other plastic materials.[9] Glass is another choice for microchip CE devices. It has the advantages of good optical transparency and clean surfaces after etching. The first microchips were developed in glass.[10] Glass can sustain high temperatures, which may be disadvantageous when sealing two glass plates, because high temperatures can destroy any integrated temperature-sensitive materials.[11]

PMMA cannot transmit wavelengths shorter than 280 nm and glass filters out wavelengths shorter than 300 nm. Thus, a 266 nm UV laser is not suitable for on-column detection on either substrate. However, one can use a laser either at 488 nm for labeled biomolecules or at 532 nm for native TPE of biomolecules to overcome this problem.

This chapter reports the application of the previously-described two-photon microscope detector to microchip CE. First, a diagnostic experiment using a conventional PMMA chip was performed. Because the laser used in TPE was too powerful to work in the normal detection scheme, which requires detection through the PMMA of the substrate, a novel detection scheme was invented. In this new design, detection was conducted through the buffer at the end of a vertical channel. Finally, a glass chip, chosen as an alternative to the PMMA chip, was successfully incorporated into the detector. Two amino acids, driven through the channel by CE, were individually detected using the two-photon microscope.

4.2 Experimental Section

4.2.1 Microfabrication of PMMA Chips

PMMA microchips were made following the method described by Kelly.[12] Briefly, to develop a silicon template, a silicon wafer was first photolithographically patterned in a clean room and then wet chemically etched by exactly following the procedure listed in reference 12. After that, in order to imprint the raised features from the Si template into the PMMA substrates, the template and substrate were placed between two clean glass

microscope slides. The microscope slides holding the PMMA and Si were screwed between two aluminum blocks to prevent the interior pieces from sliding. The entire assembly was placed in a preheated oven at 105°C for 5 min to soften the PMMA. After the assembly was momentarily removed from the oven, eight screws in the aluminum plates were tightened and the package was returned to the oven for another 5 min followed by cooling down to 90°C. Thus, the channels were formed in the PMMA substrates.

Two channel patterns were made by using the method described above. One was a conventional double-T injector design and the other was a novel custom-made design. This new design was created after it was determined that there were problems associated with the conventional design. Before imprinting the custom-made channel pattern into the PMMA substrates, four holes were already drilled halfway through one long edge of the PMMA by a CO_2 laser cutter (C-200, Universal Laser Systems, Scottsdale, AZ). These holes served as half of the reservoirs. The other half of the reservoirs were drilled in a blank PMMA substrate. For the conventional double-T design, reservoir holes were only drilled in a blank PMMA.

For bonding the imprinted PMMA with the blank PMMA, microscope slides and two stainless steel plates were used to sandwich the substrates in the same way as in imprinting except five C-clamps were used. When pressure was applied on the C-clamps, the slides and plates transferred the pressure to the substrates to tighten them. Extra care was essential to precisely align the two reservoir halves in the custom-designed chip. The

entire package was then placed in a preheated oven at 96°C for 32 minutes and cooled down to 28°C. Figure 4-1 (a) and 4-1 (b) show pictures of custom-made and conventional PMMA chips, respectively.

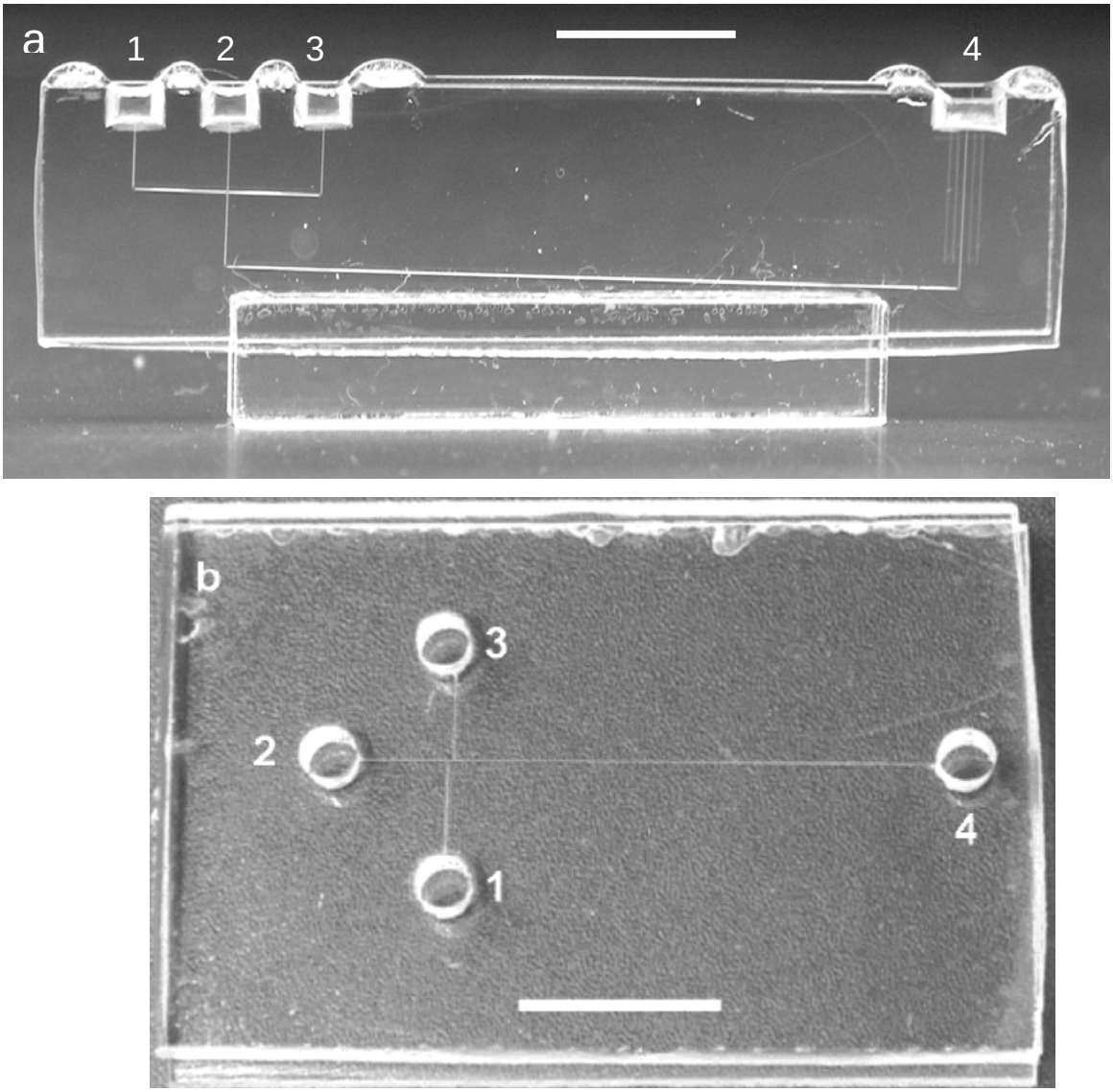

Figure 4-1. Photographs of completed custom-made (a) and conventional (b) PMMA chips. Reservoirs 1-4 in both pictures represent analyte reservoir, buffer reservoir, analyte waste reservoir, and waste reservoir, respectively. In (a), the channel lengths from reservoirs 1-4 to the injection intersection were 0.8 cm, 0.3 cm, 0.8 cm, and 4.6 cm, respectively. In (b), the channel lengths from reservoirs 1-4 to the injection intersection area were 0.5 cm, 0.5 cm, 0.5 cm, and 2.2 cm, respectively. The double-T injection intersection was offset by 200 μm. Scale bars represent 1 cm in both pictures. Picture (b) is from Ref. 12.

4.2.2 Glass Chip and Chemicals

The glass microchip was purchased from Micralyne (Alberta, Canada). It was made from low-fluorescence Schott Borofloat® glass and had a double-T injector design like that in Figure 4-1 (b). The dimensions of the chip were 16 mm×95 mm×2.2 mm. The channel lengths from reservoirs 1-4 to the injection intersection were 0.8 cm, 0.8 cm, 0.8 cm, and 8 cm, respectively. The arms of the double-T junction were offset by 100 μm to define the injection volume. The channel was 20 μm deep and 50 μm wide at the top. At the end of each channel were 1.1 mm deep access holes with 2 mm diameter.

In the conventional PMMA chip experiment, a pH 7, 10 mM phosphate buffer was used. The phosphate buffer was made in the same way as that described in Chapter 2. In the CE test experiment using the custom-designed PMMA chip, 100 μM sodium fluorescein was made from fluorescein powder (Sigma, St. Louis, MO) and sodium hydroxide pellets (EMD, Gibbstown, NJ) dissolved in pH 8.7, 10 mM Tris buffer containing 0.5% (w/w) hydroxypropyl cellulose (HPC; average MW 100 000; Sigma-Aldrich, St-Louis, MO). The buffer was made from Trizma HCl and Trizma Base (Sigma, St-Louis, MO) dissolved in 18 MΩ water from a Milli-Q water system (Millipore, Billerica, MA). The HPC was to minimize electroosmotic flow and analyte adsorption to the channel walls.[15] In the CE experiment with the custom-made PMMA chip, 1 mM tryptophan (Matheson, Coleman & Bell, Norwood, OH) was made in the same Tris buffer. The Tris buffer was also used as the run buffer for CE. In the CE experiment with the glass chip, 1 mM tryptophan and 5 mM tyrosine (ICN Biomedicals, Irvine, CA) were

prepared in pH 4, 10 mM acetate buffer, which also served as run buffer for CE. The buffer was prepared from glacial acetic acid (Mallinckrodt Baker, Paris, Kentucky) and sodium hydroxide pellets (EMD, Gibbstown, NJ) dissolved in Milli-Q water. All solutions were passed through 0.2-μm filters (Whatman, Florham Park, NJ) prior to use.

4.2.3 Exploratory Experiments with the Laser

First, the channel of the conventional PMMA chip (Figure 4-1b) was filled with phosphate buffer. A 15 μl volume of the buffer was pipetted into reservoirs 1, 2, and 3. In this way, the channels were automatically filled with buffer. Reservoir 4 was then filled by pipetting another 15 μL of the buffer. After filling, the chip was placed under white light of the microscope with the visible cube employed. With the laser turned on, one was able to view through the eyepiece and monitor the adjustment of the laser position and focus. By tuning the stage and the coarse and fine knobs of the microscope, the smallest laser spot was focused inside the channel.

The laser often burned holes in the microchip after focusing the laser spot, to investigate this problem, a small piece of fluorescent plastic was sanded on one surface to make it rough for better light contrast. This rough surface was then exposed to the laser. By turning the fine knob of the microscope, which changed the vertical distance between the plastic and the UV-achromatic microscope objective, the rough surface was moved toward the objective. During this movement, the laser was allowed to shine on the rough surface of the plastic under the two-photon cube for 60 seconds after each 10 μm

adjustment in distance. For each subsequent 10 μm adjustment, a fresh location on the plastic was exposed to the laser. A total of 10 points, including the focal point of the laser focused by the objective, was obtained, translating to 100 μm in vertical distance. The rough surface was then examined by a 40× DL objective on a Nikon microscope. The size of focal point was estimated by comparison to a USAF 1951 resolution test target.

4.2.4 CE Test Using Custom-designed PMMA Chips

As shown in Figure 4-1(a), the custom design had 4 reservoirs on one of the long edges of the chip. When used in CE, the chip stood on the other long edge; thus, the channel was on the vertical plane and the reservoirs were aligned linearly on the top. This design enabled detection through the buffer in reservoir 4 instead of through the PMMA substrate.

A simple experiment was designed to see if CE could operate with such a channel layout. A blue light-emitting diode (LED) served as the light source to excite the native fluorescence of sodium fluorescein, a dye that gives bright-yellow fluorescence under blue light. A solution of 100 μM sodium fluorescein was considered as the sample in this experiment and the Tris buffer served as the run buffer.

Prior to running CE, the channels were filled with pH 8.7, 10 mM tris buffer containing 0.5 % HPC as described in Section 4.2.3, except that 20 μL of the buffer was pipetted into each reservoir. Then, vacuum was applied to reservoir 1 to remove the buffer, and 20 μL of 100 μM sodium fluorescein was added by pipet. Four platinum wires

were inserted into the reservoirs serving as electrical contacts. Two power supplies (PS350/5000V-25W, Stanford Research Systems, Sunnyvale, CA) provided injection and separation voltages. A home-built voltage-switching box (Instrument Shop at Brigham Young University, Provo, UT) allowed fast switching between the injection and separation potentials.

The blue light from the LED was then directed on the chip. A "pinched" injection method[13] was used in this experiment and in all CE experiments in this chapter. This method prevented diffusion of sample into the separation channel and provided an injection volume which was independent of sampling time. For injection, +600V was applied to reservoir 3 for 30 s, while reservoirs 1, 2, and 4 were grounded. During separation, +2000V was applied to reservoir 4, with reservoirs 1 and 3 being maintained at +600V and reservoir 2 grounded. The bright-yellow fluorescence was very visible to the naked eye, so one could easily observe the sample when it was moving inside the channel. The two-photon microscope was not employed in this experiment.

4.2.5 Microchip CE Using Custom-designed PMMA Chips

The Tris buffer having 0.5 % HPC (w/w) was pipetted into the channels of the chip. Buffer in reservoir 1 was removed and 20 µl of 1 mM tryptophan was pipetted in.

At first, the visible cube in the microscope was used to enable viewing of the laser focus inside the channel. After the laser was focused, the microscope was switched to the two-photon cube with which CE was performed. Sample injection and separation

procedures were exactly the same as those in the CE test experiment.

For detection, the laser penetrated through buffer in reservoir 4 and was focused on the bottom of the reservoir by observing through the eyepiece under the white light of the microscope with the visible cube in place. With careful tuning of the translation stage, the laser spot could be moved to the end of the channel, where one could not see the laser spot anymore. Detection was performed at that point. Then the two-photon cube was switched in position. Signal, collected by the PMT, was first amplified by an amplifier, which was connected through a coaxial delay line to a gated photon counter. Data were acquired with Labview software running on a Dell personal computer.

4.2.6 Microchip CE Using Glass Chips

The acetate buffer was injected into the channels of the glass chip by the method described in Section 4.2.3, except that 4 μL of buffer were pipetted into each reservoir. After removing the buffer in reservoir 1, 4 μL of 1 mM tryptophan or 5 mM tyrosine were introduced.

Sample injection and separation procedures were the same as those in the CE test experiment except that the injection voltage was set to -600 V and the separation voltage was set to -2000 V in this experiment. Detection was performed on the separation channel, 5 cm away from the injection junction. Signal collection and processing was the same as in the above experiment. The counting cycle of the photon counter was set to 3000. With

the 7.75 kHz repetition rate of the laser trigger, the integration time for each data point thus was 0.39 second.

4.3 Results and Discussion

4.3.1 Effect of High Laser Power on PMMA

When the laser beam was focused inside the channel of a conventional PMMA chip, it burned a hole in about 10 s. This was repeatedly observed wherever the laser was focused on a new place of the channel. Therefore, a series of burned holes at different distances were obtained, whose linear arrangement showed an hour-glass shape. The focused laser spot was located at the thinnest part of the hour-glass. This spot, measure by the resolution test target, was 5-μm in diameter, which was larger than the theoretical 1-μm focal point of the UV-achromatic objective found in the manual of the objective. In practice, the spot size should be limited by diffraction. The minimum size of the spot formed at the focus of the objective is defined by[14]

$$d = 2.44\lambda\frac{f}{a},$$

where λ is the wavelength of the beam, *f* is the focal length of the objective, and *a* is the diameter of the beam. In our case, when the collimated 532 nm laser beam with a diameter of 4 mm was focused through the 10 mm focal length objective, the diffraction limited spot formed at the focal point of the objective was calculated to be 3.2 μm. In this experiment, the rough surface of the plastic may not be an ideal object because of

insufficient contrast. The contour of the spot viewed under a microscope was determined more subjectively than objectively by the researcher. All of these contributed to the discrepancy between the measured and calculated values.

However, both values were smaller than the channel size, which was a trapezoid with 80-μm width at the top, 40-μm width at the bottom and 30-μm height. Since the two-photon events only took place at the focal point, where the laser was most intense, the laser light inside the channel should not cause burning of PMMA.

After studying the whole series of holes burned on the rough plastic surface, it was clear that not only the focal point but also all cross sections in the laser's hour-glass like profile had a high enough power to burn the PMMA surrounding the channel. Although the burning threshold in distance from the focal point was not studied, the already studied 100-μm depth of the laser was far greater than that of the channel. Given that the burning of the PMMA was caused by the laser, the two-photon detector could not be used with the conventional chip geometry. Thus, a novel custom-designed detection scheme was invented.

4.3.2 Laser Focus Problem Using Custom-designed PMMA Chips

Compared to CE on conventional chips, CE performed on this novel chip [Figure 4-1(a)] caused the sample to flow against gravity in some regions of the channel. However, for such small volume, the electric field force was greater than the force of gravity. The effect of gravity on the fluid was negligible. By following the experimental

procedures listed in Section 4.2.4, it was observed that sample could be injected very well and a small plug migrated quickly from the injection cross to the detection reservoir during separation.

When performing CE on this chip, nothing was detected by the two-photon microscope. The microscope had a detection limit of ~1 μM for tryptophan in a 1-mm flow cell. Since concentrations as high as 1 mM were used, and CE was demonstrated to work on this chip, the problem could not have been caused by inadequate sensitivity of the detector.

In addition, detecting through the buffer should not be much different from detecting through the PMMA from the standpoint of refraction of the laser light. Since the PMMA has a refractive index of 1.492 at 589.3 nm and the buffer, if assumed to have the same refractive index as water, has an index of 1.33, there only would be ~10 % difference in refracted light passing through these two media.

During the experiment, it was found that factors associated with laser focusing hindered successful detection. These included the roughness of the reservoir bottom, where the channel ended and the laser was focused, and the irregularity of the shape of the channel end. The rough surface of the reservoir bottom caused strongly scattered light, making it difficult to observe the focusing of the laser spot. An irregularly shaped channel end was hard to find under the microscope, not to mention focusing the laser in it. All of these problems rose from poor manufacturing of the chip during imprinting and bonding. Clogging of the channel happened as well when bonding two pieces of PMMA together.

A more careful and professional manufacturing process might improve these problems.

It was also found that when the laser was irradiating through the buffer in the reservoir, the heat generated by the high power of the laser evaporated the buffer gradually. Because the changing buffer surface was changing the refraction of the laser beam, the laser was no longer focused at its original position. As a result, the focus of the laser changed during CE. This was the most challenging problem. To overcome this, a small piece of thin glass slide was used to cover the top of the waste reservoir, only leaving a small space to allow the platinum wire to fit. However, it was observed that during the experiment, a small bubble was formed in the space. The bubble, caused by evaporation of the buffer, changed the focus of the laser by changing the refractive index of the medium in which the laser was traveling. This method did not solve the problem, but it was an appropriate direction in which further efforts should be made.

4.3.3 CE Results Using Glass Chips

Figure 4-2 shows transmittance curves of Borofloat® glass, from which the glass chip was made, in the UV range. The top cover of the chip used in this study was 1.1 mm thick, which corresponds to curve 2 in the figure. As discussed in Chapter 2 of this thesis, tryptophan, tyrosine, and phenylalanine had TPE fluorescence wavelengths centered at about 380 nm, 310 nm, and 275 nm, respectively. Reading from curve 2, the transmittance of the glass at these three wavelengths was about 90%, 85%, and 30%, respectively. Because the TPE fluorescence of phenylalanine was poorly transmitted by

the glass, it was not employed in this study.

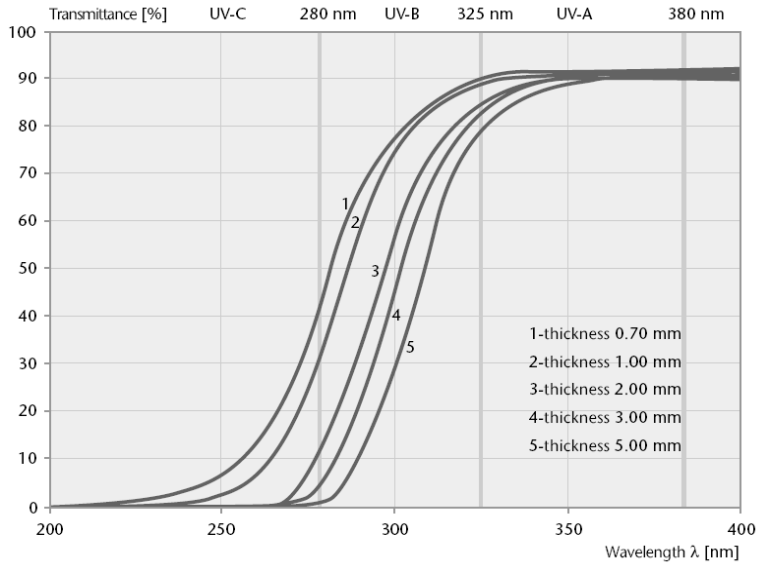

Figure 4-2. Transmittance curves for BOROFLOAT® glass in the UV range (from Ref.15).

Tryptophan and tyrosine were chosen to test the performance of the two-photon microscope detector for micro-scale separation on the glass chip. The isoelectric points for tryptophan and tyrosine are 5.89 and 5.66, respectively. In pH 4 acetate buffer, both of them were positively charged. Because the glass chip was used without any treatment on the inner surface of the channel, eletroosmotic flow (EOF) occurred when the voltage was applied, and the positively charged analytes moved in the same direction as the EOF. Therefore, a negative voltage was applied in both sample injection and separation modes.

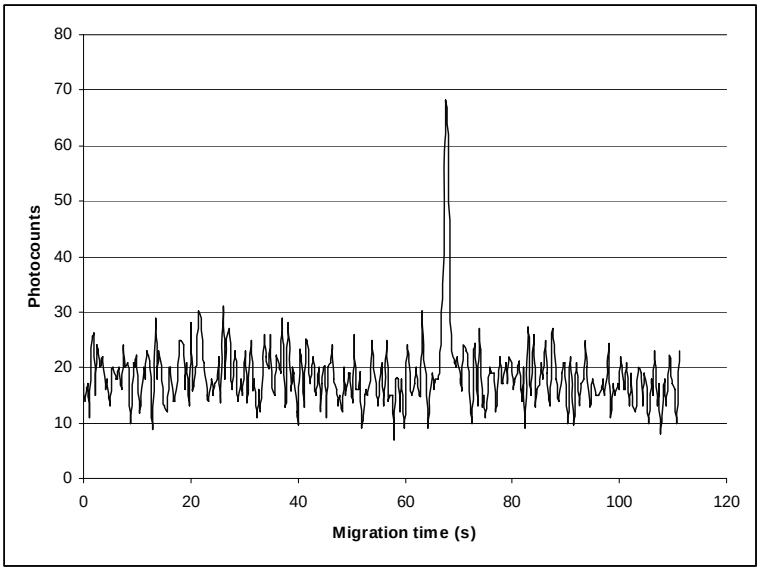

Figure 4-3. Electropherogram of 1 mM tryptophan on a glass chip. Experimental conditions were described in Section 4.2.6. The data were recorded at 2.56 Hz.

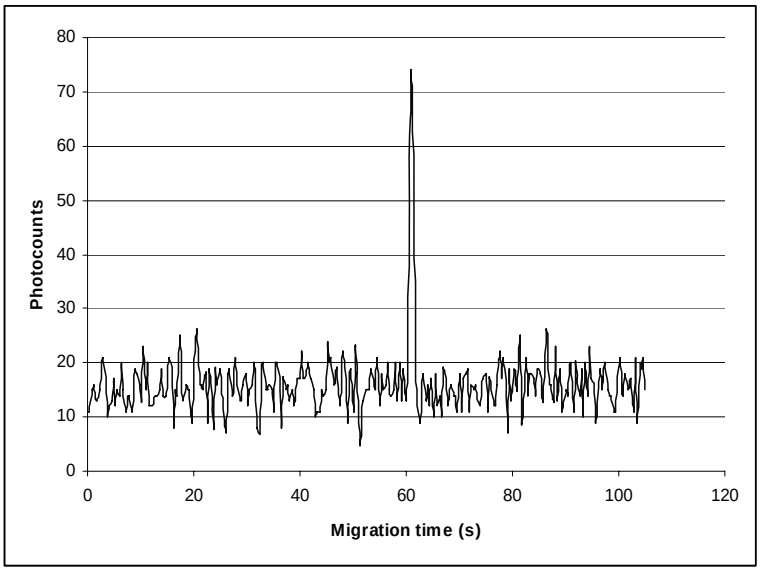

Figure 4-4. Electropherogram of 5 mM tyrosine on a glass chip. Experimental conditions were described in Section 4.2.6. The data were recorded at 2.56 Hz.

Figures 4-3, 4-4 depict electropherograms of tryptophan and tyrosine, respectively. Having a similar mass-to-charge ratio, tryptophan and tyrosine had close retention times at 67 s and 61 s. The calculated theoretical plate numbers for the peaks of tryptophan and tyrosine are 18 000 and 20 000, respectively. The lower signals obtained in this experiment than those in a flow cell were caused by the poor optical quality of the glass chip and diffusion of the injected analytes.

During CE, the photon counter was set to integrate the signal every 0.39 s, which meant that data were recorded at a rate of 2.56 Hz. In theory, the signal could be recorded on the time scale of the interval between laser shots. However, the faster the signal was recorded, the lower the signal-to-noise ratio would be. As a compromise, a counting cycle of 3000, related to the laser's repetition rate of 7.75 kHz, was set for the photon counter to integrate the signals. In the experiment of separating tryptophan and tyrosine in a square capillary described in Section 2.2.3, the photon counter was set at a 0.5 s integration time, which contributed to the higher signals obtained than this experiment.

4.4 References

1. Harris, D.J., Fluri, K., Seiler, K., Fan, Z., Effenhauser, C.S., Manz, A. *Science* **1993**, *261*, 895-897
2. Zeng, Y., Chen, H., Pang, D., Wang, Z., Cheng, J. *Anal. Chem.* **2002**, *74*, 2441-2445
3. Qin, J., Fung, Y., Zhu, D., Lin, B. *J. Chromatogr. A* **2004**, *1027*, 223-229
4. Schulze, P., Ludwig, M., Kohler, F., Belder, D. *Anal. Chem.* **2005**, *77*, 1325-1329

5. Uchiyama, K., Nakajima, H., Hobo, T. *Anal. Bioanal. Chem.* **2004**, *379*, 375-382

6. Okerberg, E., Shear, J. *Anal. Chem.* **2001**, *73*, 1610-1613

7. Zugel, S., Burke, B., Regnier, F., Lytle, F. *Anal. Chem.* **2000**, *72*, 5731-5735

8. Boone, T.D.; Fan, Z.H.; Hooper, H.H.; Ricco, A.J.; Tan, O.H.; Williams, S.J. *Anal. Chem.* **2002**, *74*, 78A-86A

9. Bayer, H.; Engelhardt, H. *J. Microcolumn Sep.* **1996**, *8*, 479-484

10. Harrison, D.J.; Manz, A.; Fan, Z.; Lüdi, H.; Widmer, H.M. *Anal. Chem.* **1992**, *64*, 1926-1932

11. Bruin, G. *Electrophoresis* **2000**, *21*, 3931-3951

12. Kelly, R.; Woolley, A. *Anal. Chem.* **2003**, *75*, 1941-1945

13. Jacobson, S.; Hergenroder, R.; Koutny, L.; Warmack, R.; Ramsey, J. *Anal. Chem.* **1994**, *66*, 1107-1113

14. http://en.wikipedia.org/wiki/Diffraction Accessed July 26, 2006

15. http://www.us.schott.com/hometech/english/download/transmit_uv_range.pdf Accessed July 26, 2006

Chapter 5

Conclusions and Recommendations

5.1 Conclusions

This thesis represents work on designing and testing an inexpensive protein detector based on two-photon excited native fluorescence of aromatic amino acids. This detector is compatible with the concept of the relatively new μTAS or "lab-on-a-chip" devices.

5.1.1 Prototype Two-photon Detector

First, a prototype two-photon detector was examined. The source of the background was confirmed to be the 355 nm radiation from the laser. A long pass filter was used to eliminate this background. Elimination of the background improved the detection limits of tryptophan, tyrosine, and phenylalanine by a factor of 4, 3, and 6, respectively, under static flow conditions. A detection limit of 130 nM was obtained for a protein, BSA, under pumped flow conditions. As evidence of the utility of this detector in micro-scale detection, simple CE was performed using a square fused silica capillary. A mixture sample containing two amino acids, tryptophan and tyrosine, was separated under 10 kV separation voltages. These two amino acids were detected with a signal-to-noise ratio of 30 and 15, respectively. The success of this prototype proved the feasibility

of building a compact and inexpensive two-photon fluorescence detector based on a microchip laser.

5.1.2 Two-photon Microscope

Using the experience gained from the prototype detector, a two-photon microscope detector was set up on the frame of a commercial Olympus microscope. The most important change made on the frame microscope was the removal of a glass compensator from the trinocular cube, which enabled UV detection. A detection limit of 790 nM for tryptophan was achieved by using a reflective objective under pumped flow conditions. This microscope detector adopted the same optical principle as the prototype, but its eyepiece provided a way to view the location where the laser was focused. The ability to view the focus of the laser was essential to apply the detector to a microchip separation device.

5.1.3 Coupling the Two-photon Microscope to Microchip Separation Devices

Finally, the application of the microscope detector to microchips was tested. PMMA chips with double-T injectors were employed initially. However, the high power of the laser destroyed the channel in several seconds by melting the PMMA. This meant that the normal detection scheme of shooting a laser through the chip substrate was not practical with this laser. A PMMA chip with a novel detection scheme was then tested. On this chip, detection was performed inside the reservoir. After exploring this detection

scheme, it was found that difficulty of obtaining a precise focus led to the detection failures. Although attempts were made, the problem was not solved in the time available. This detection scheme is still believed to be an effective solution to the coupling of PMMA chips with two-photon detection. Thus, further study on this issue is advised. Finally, a glass chip was chosen as an alternative to PMMA to complete the task of two-photon detection on microchips. Single aromatic amino acids were successfully detected by the two-photon microscope after CE on the microchips.

5.2 Recommendations

In Chapter 3 it was found that signal-to-noise of the two-photon microscope reached its maximum when the iris aperture was left at 2.5 mm. After collection by the objective, the fluorescence should be collimated. The collimated beam should then focused into a fine spot by the tube lens. However, the 2.5 mm size of the iris aperture used in my experiments means that image of the focused laser spot had a relatively large size. The abnormal size of the laser focus spot may be caused by poor wavelength match of the laser radiation with the design of the objective, leading to different focal points for the laser and the fluorescence. Because of the difference in focal points, the fluorescence was not perfectly focused into a small spot. To improve the laser focus image quality, an objective whose design wavelength includes the 532 nm laser wavelength used in this research should be employed. Better focusing of the fluorescence at the iris could lead to better background rejection and improved detection limits.

In Chapter 4 a novel PMMA microchip was described. Although successful application of the chip was not achieved at the time this thesis was completed, it is believed that with further improvements, the chip can be incorporated into the two-photon detection system. Improvements should focus on overcoming the changing level of buffer in the detection reservoir as a result of buffer evaporation. A small piece of thin glass slide was a good try since it produced a flat instead of a curved surface and minimized the effect of light scattering. However, it didn't solve the problem of changing height of the liquid because bubbles formed under the glass slide. More effort should be made to design a closed detection reservoir with a more suitable cover to prevent evaporation of the liquid. One possibility is sticking a thin glass slide over the top of detection reservoir, with a small hole drilled through the glass slide to allow for the passage of the electrical wire. With no extra space in between the glass slide and the detection reservoir, bubbles will not form. The success of this method depends on high-quality manufacturing of the reservoirs, since the two half reservoirs need to be as flat as possible after they are bonded together.

The detection of proteins in analytical separation was not studied in this thesis. With further optimization of chip layout and laser focusing, the two-photon detector can be useful for protein analysis on PMMA microchips.